JOINT EUROPEAN TORUS

JET–P(90)52

R.S. Hemsworth, A.J.T. Holmes
and JET Team

High Energy and High Power Ion and Neutral Beam Source Development

High Energy and High Power Ion and Neutral Beam Source Development

R.S. Hemsworth, A.J.T. Holmes[1]
and JET Team*

JET-Joint Undertaking, Culham Science Centre, OX14 3DB, Abingdon, UK

[1]AEA Technology, Culham Laboratory, Abingdon, Oxon, OX14 3DB
** See Appendix 1*

Preprint of Paper to be submitted for publication in
BNES

HIGH ENERGY AND HIGH POWER ION AND NEUTRAL BEAM SOURCE DEVELOPMENT

R S Hemsworth[1] and A J T Holmes[2]

1. Introduction

With the stimulus of the requirement for high power, high energy hydrogen ion beam sources as the basis of neutral beam injectors for fusion research, the development of such sources over the past two decades has been quite spectacular. This article briefly explains the background to this work and reviews the development that has taken place within the UK, which has played a prominent role throughout this period.

2. Background

For many reasons, ion beams have been studied and developed throughout the world for many years, and at least one authoritative review covers the development until 1974 [1]. This article reviews progress since the early 1970's, with particular emphasis on the development within the UK.

2.1 The Reason for Ion Beams in Fusion Research

It has been accepted within the fusion research community since the 1960's that some form of "additional heating" is required to raise the temperature of a magnetically confined plasma to levels where significant fusion reactions occur. One simple idea is to inject a high energy neutral beam, with the same nucleus as the plasma ions, across the confining magnetic fields. Once inside the plasma, the beam is readily ionised; it is then trapped by the magnetic field and gives its energy to the plasma via collisions. The neutral beam is created by the neutralisation of an ion beam which has been accelerated to the desired energy.

---

1 JET Joint Undertaking, Abingdon, Oxon, OX14 3EA, UK

2 AEA Technology, Culham Laboratory, Abingdon, Oxon, OX14 3DB

2.2 Beam Composition

The most promising fusion plasma ions are the two heavy isotopes of hydrogen, deuterium and tritium. In order not to pollute the plasma, the beam has to consist of the same species. For reasons of economy and the avoidance of neutron production by fusing plasma ions, hydrogen was used in most experiments and their associated beam systems in the 1970's. Throughout the 1980's D^+ ions were required, hence discharges in deuterium gas were used. As already mentioned, fusion reactor plasmas are likely to be a D^+/T^+ mixture, but is is unlikely that tritium beams will be used.

The sources used to date have been positive ion sources. These produce three separate ion species, H^+, H_2^+ and H_3^+. (Their isotopic counterparts are produced if the appropriate gas is used. This applies to all the following discussion, unless specifically stated otherwise.) Future systems will be based on negative ion sources (see 2.3 and 4 below). Only the single negative ion species exists, H^-.

2.3 Beam Energy

The desired energy is set by two main requirements. First, and most obvious, the beam energy must be substantially above that of the average ion in the target plasma. Secondly, the beam has to give up its energy to the plasma in the right place, which is near the centre rather than at the edge. The combination of these two requirements demanded beam energies of ~ 20 keV/nucleon in 1973. As the target plasmas became hotter, denser and larger, the required energy rose to ~ 80 keV/nucleon in the 1980's. A new requirement, to drive current within the toroidal confinement devices planned for the next step in fusion research, demands energies of > 500 keV/nucleon.

Neutralisation of positive ion beams by simple electron capture from a gas (H_2) target is relatively efficient at low energies, < 80 keV/nucleon. However the neutralisation process is a very strong function of energy, as shown in Fig.1 [2], and it becomes unrealistic, and uneconomic, to use positive ion beams at high energies > 100 keV/nucleon. This is not the case with negative ions, where neutralisation by either a gas or plasma target

is essentially independent of the beam energy from 20 keV/nucleon to many MeV/nucleon (~ 60% for a gas target, and ~ 80% for a plasma target).

The relative ease of creation of positive ions and the aforementioned energy considerations have meant that they have formed the basis of all neutral beam systems to date. The high energy demanded for future current drive systems means that they will be based on negative ions.

2.4 Pulse Length

The time for which the beam is required was set in the early experiments to several times the energy confinement time for the fusion plasma. Typical confinement times in the experiments of the 1970's were ~ 10 mS, so that pulse lengths of < 100 msec were the normal requirement. The latest generation of devices, such as the JET tokamak, have energy confinement times as long as 1 sec, and beam pulse lengths of ~ 10 sec are needed. If neutral injectors are use to drive the current in the next step fusion devices, the sources will have to be capable of continuous operation, with pulse on times of up to 2 weeks.

3. Positive Ion Sources

As electrostatic acceleration is the simplest and most efficient method of obtaining the required beam energy, this has been chosen for all positive ion based neutral beam systems: A flux of ions arriving at an aperture in an electrode are accelerated towards a second electrode at a lower potential, through which they pass to form the beam. There is no equivalent of a thermionic electron emitter in the world of positive hydrogen ions, and the source of ions is usually a plasma source connected directly to the accelerator.

3.1 Ion Optics

Confusion often arises in the names given to the grids of an ion extraction system. For the rest of the discussion on positive ion systems, the grid in contact with the source plasma will be referred to as the plasma grid and the last grid as the ground grid. (It is most common to run a positive ion extraction system with the plasma source at the requisite high

positive voltage, with the last grid at ground potential. However, it is possible, and indeed systems have been operated, with the plasma grid at ground with the last grid at a high negative potential.) The electron suppressor grid will be termed the suppressor grid. In the discussion on four grid systems, when an additional grid is introduced between the plasma and suppressor grids, this will be called the gradient grid.

Multi ampere beams appeared quickly once it was realised that the key to both high current and high quality (low divergence) beams lay in the understanding of the electrostatic optics. The ion optics of an extraction system have been described in detail elsewhere [3], and are only briefly reviewed here. There are two significant effects:

First, an aperture in a metallic electrode with a different electric field each side of the electrode acts as a lens for ions passing through that aperture. If space charge effects are ignored, then the focal length, f, of the lens is given by

$$f = \frac{4\,V}{(E_2 - E_1)} \qquad (1)$$

where V is the energy of the ion arriving at the aperture and E_1 and E_2 are the electric field upstream and downstream of the aperture respectively. Thus with a simple two aperture accelerating system, the second aperture is a negative lens, and a parallel beam can only be achieved if the initial ion trajectories are convergent. The first aperture is neglected as a lens because the ions have essentially zero energy there, and the initial ion trajectories are determined by the shape of the plasma boundary at the emitting aperture. As a first approximation, the plasma boundary at a circular aperture may be assumed to the part of the surface of a sphere. The curvature of the boundary is controlled by the physics of the plasma and of the acceleration region, ie. the rate of arrival of ions at the boundary, the need to conserve current during acceleration, Poisson's equation, and the rate of change of momentum set by the accelerating field. For a given accelerator geometry and acceleration potential, the curvature of the plasma boundary is determined only by the rate of arrival of ions at the boundary, and thus there

is only one value of ion current that gives a parallel beam. If the ions are of mass A in a.m.u., this is given by:

$$I = 1.72 * 10^{-7} * \frac{a^2}{d^2} * \left[1 - 1.6 * \frac{d}{r_c} \right] * V^{3/2} * A^{-1/2} \qquad (2)$$

where a is the aperture diameter, d is the accelerating gap, and r_c is the radius or curvature of the plasma boundary. Green [1] has shown that the term in brackets in equation (2) has the value of 0.66 for collimated beams.

Secondly, it is found that to obtain a low divergence requires:

$$\frac{a}{d} < 0.6 \qquad (3)$$

As d has a lower limit where the accelerating voltage will cause a flash over, the current from a single aperture is limited. A practical limit to the electrical stress in the accelerating gap is 10 kV/mm.

It is fairly easy to demonstrate that with the restrictions imposed by the criteria given above, the current density from a single aperture is limited to ~ 2.5 kA/m^2, and the current from a single aperture is limited to < 200 mA. To obtain higher currents, "beamlets" from many parallel apertures in each electrode are amalgamated to form the required beam.

Obviously all the beamlets have to be directed in exactly the right way to obtain the required beam, and therefore the apertures have to be geometrically accurate. Additionally, as the apertures form lenses, if a beamlet were to enter the aperture off axis, it would be deflected. This effect can be made use of in focusing all the beamlets to some desired point. It is known as offset aperture steering.

Although it is mentioned above that a parallel beamlet is obtained if the correct ion flux is delivered to the extraction aperture, this is not the case in practice. Additional effects, not mentioned above, all of which increase the beamlet divergence, are the finite temperature of the ions, aberrations

arising from imperfect electrodes, space charge effects, and non uniform illumination of the aperture, either temporal or spatial.

As already mentioned, there is a lower limit to the size of the gap set by flashover between the two grids. During the early development of ion sources, experimental data [3] set this limit as

$$V_b = 6 * 10^4 * d^{1/2} \qquad (4)$$

where V_b is the voltage at which breakdown between the grids will occur. It is obvious from equation 3 that high currents could not be obtained from a simple single gap accelerating structure. It was suggested that this limitation could be overcome by having more than one accelerating gap [4]. In this case, the first extraction gap determines the current, and the subsequent gap(s) the beam energy. Of course, each gap will act as an electrostatic lens, and this actually allows a greater control over the beam optics. (As will be described below, it has now been shown that equation 3 does not apply at higher voltages.)

3.2 Electron Suppression

In practice a positive ion acceleration system has to have a minimum of three electrodes, rather than the two discussed above. In a neutral injector, it is convenient, and usual, to use the same gas in the neutralising gas cell as in the ion source. Therefore, use is made of the gas from the ion source by having the neutraliser closely coupled to the exit of the accelerator. In addition to the neutralisation reactions already mentioned, many other reactions occur between the beam and the target gas, not least the simple ionisation of the target gas. This means that the beam creates a second plasma in the neutraliser. (Even if the neutraliser were not closely coupled, there will inevitably be some plasma created as a gas target must exist immediately downstream of the accelerator as a result of the gas flowing from the ion source.) Thus with a simple two electrode accelerator, not only would positive ions be extracted from the plasma source, but electrons would also be extracted from the neutraliser plasma, and be accelerated back into the plasma source. Although the density of the plasma in the neutraliser is typically of the order of 1% of that in the plasma source, as electrons are

much more mobile than ions it is easy to obtain backstreaming electron currents equal to the extracted ion current. This would give both unacceptable power loads on the plasma source, and greatly reduce the overall efficiency of the system.

The solution has been to introduce an additional electrode upstream of the last grid, the electron suppressor grid, which is held at a negative potential relative to the beam plasma. This is shown schematically in Fig.2. The voltage of this grid is set such that the potential at the beamlet axis is sufficiently negative to suppress electron extraction from the neutraliser plasma. Inevitably ions are then extracted from the weak neutraliser plasma, but the ion current is low, and they are only accelerated as far as the suppressor grid as they are then repelled by the field in the extraction gap. These ions are collected by the suppressor electrode. The overall result is a low current, and a low power to the suppressor electrode, with little reduction in system efficiency.

3.3 Plasma Source Requirements

An ideal plasma source would be of simple construction, easy to operate, tolerant of variations in gas and electrical supplies, have a high electrical efficiency, and operate at low gas pressure. The physics of the beam system and the fusion plasma make additional demands. As is pointed out in 3.1 above, there is only one value of ion flux to an extraction aperture that results in a parallel beamlet, and that high currents can only be obtained by having multi aperture extraction systems. These two requirements mean that the plasma has to provide the same ion flux to each aperture, ie. over a large area. There are, however, several other requirements that must be simultaneously met. Although not discussed in detail, the various restrictions on the plasma source are given below, and typical requirements indicated.

3.3.1 Gas Efficiency

3.3.1.1 Paschen Breakdown

The plasma source is connected directly to the extraction system, so any gas introduced into the ion source will flow through the extraction system to

the vacuum pumps. As high electric fields exist in the acceleration stack, the pressure there must be either sufficiently low or high to avoid creating a cold cathode discharge, ie. "Paschen breakdown". As is discussed below, only operation at low pressure is possible, hence the source gas efficiency has to be high, and the plasma source must operate at low pressure. Given the required electric field (see 3.1), the pressure in the accelerator has to be < 0.5 Pa, and the plasma source has to operate at a similar pressure.

3.3.1.2 Backstreaming Electrons

As the extracted beam is being accelerated, some ionisation of the gas in the accelerator will occur. Ionisation creates electrons in this region, which will be accelerated back into the plasma source, which could create high power loads within the source. Some of these backstreaming electrons may also hit the acceleration grids, dumping power into those grids. Additionally, the ions created will be accelerated, but not to the full energy, and they will be divergent as they will not have the same starting point in the overall optics as the extracted ions. Thus such ionisation results in a current drain on the high voltage supply (reducing the system efficiency), and power loading on the plasma source and the accelerator grids. Examination of the cross sections involved sets the level for the pressure in the accelerator at < 0.5 Pa, a similar value to the Paschen limit.

3.3.2 Plasma Uniformity

As already mentioned, the plasma source must give a uniform flux of ions to the extraction grid in order to obtain a low divergence beam. This is also necessary in order not to misdirect individual beamlets. If the plasma is non uniform, a density gradient would exist across each extraction aperture. This would give a tilted plasma boundary across the aperture, and the beamlet will not leave normal to the grid surface, and it would not be parallel to the other beamlets, giving an increased divergence for the overall beam. The ion flux is a function of the electron temperature in the plasma, and the plasma density. However the electron temperature is usually quite constant within a plasma source, so the ion flux is, in general, proportional to the local plasma density which therefore has to be uniform. The exact uniformity requirements are set by the optics of the extraction system, but typically the uniformity needs to be within ∓ 10% over the extraction area.

3.3.3 (Beam Divergence) Ion Temperature

The minimum divergence of a positive ion beam depends largely on three factors; the temperature of the beam ions, the effective or net beam space charge and the degree of beam optical aberration. The contribution of the latter can be largely eliminated by correct shaping of the extraction electrodes, particularly the plasma grid (see section 3.4.3) but the other two can have a considerable effect. The space charge field depends on the beam current and energy (it is proportional to $I/V^{½}$) but is reduced considerably to typically 1 to 5% of its full value by slow electrons formed in the beam channel by ionisation of the background gas. As a result, the space charge and the ion temperature effects (the latter is proportional to $(T_i/V)^{½}$) although usually the former is dominant, particularly for the intense beams used for injectors [5].

Typical values for beam divergence are around 25 milliradians for 30 keV beams of which 7 to 10 milliradians may arise from ion temperature effects. At higher beam energies the divergence angle falls and at 80 keV it is around 12 milliradions.

3.3.4 Beam Species

As already indicated in 2.2, three positive ion species are produced within a hydrogen plasma, H^+, H_2^+ and H_3^+. During the passage through a neutraliser, the molecular ions are broken up to give H^+ and $H°$ at one half and one third the extraction energy. As discussed in 2.3, it is required that the beam be deposited in the correct region of the fusion plasma, and this is dependent on the beam energy. For this reason, it is quite undesirable to have the molecular ions and great emphasis has been replaced on having a plasma source that gives a high proton ratio. The demand from the present generation of fusion devices such as JET* is for > 80% protons.

---

* Joint European Torus - the worlds largest fusion experiment, situated at Culham in Oxfordshire.

3.4 UK Ion Source Development

3.4.1 The CLEO Source

The first multi ampere ion source produced in the UK was built at Culham Laboratory in 1972 [6]. This was a copy of source developed at ORNL in the USA, which used a duopigatron plasma source. Combining experience gained with that source and the sources being developed at Culham for space ion thrusters, a new source was developed which can produce a 10 A hydrogen beam [7]. This was the first UK developed multi ampere ion beam source and it formed the basis for the neutral injection system for the CLEO tokamak experiment at Culham Laboratory. The "CLEO source" operated at < 30 kV for pulse lengths of < 30 msec. The pulse length was limited by the power loading to the multi-aperture grids, which were made of copper and edge cooled. A schematic of that source and a table of its parameters is given in Fig.3.

3.5.1.1 Plasma Source

The source was cylindrically symmetric with a single directly heated tantalum wire forming the cathode. This is situated inside a soft iron "compressor". A coil around the compressor produced a magnetic field which was concentrated by the conical end of the iron compressor, from which the field expanded as indicated in Fig.3. H_2 introduced into the compressor was ionised by the thermionically emitted electrons. Two plasma regions were set up, separated by a double plasma sheath which formed at the mouth of the compressor. Electrons emitted from this sheath (referred to as primary electrons below) followed the expanding magnetic field to produce plasma over an extended area. The high energy of these electrons ensured that the plasma grid floated at near the cathode potential, indeed the source could be operated with the plasma grid connected directly to the cathode, with a slight improvement in efficiency, but an increase in temporal fluctuations on the plasma density.

The source provided plasma over the extracted area with the radial distribution of plasma density shown in Fig.4. Clearly the area within which the plasma density is uniform to within $\mp$ 10% is rather restricted. This

arose because of the presence of the magnetic field. Ions and electrons are lost at the walls and the anode, the latter collecting a net electron current equal to that leaving the cathode. These losses create a plasma density gradient, and particles diffuse down this gradient, across the magnetic field to the walls, balancing the creation by the primary electrons in the source volume. The magnetic field restricted the particle flow, and consequently the plasma density gradient was relatively steep. The adverse effect of this variation in plasma density on the beamlet divergence was avoided as indicated below.

3.4.1.2 Extraction System

The extraction system consisted of 3 circular copper grids, 80 mm in diameter, each with 349 identical cylindrical apertures. The aperture diameters and the average grid spacings were as indicated in Fig.3. As pointed out above, to ensure the beamlets all emerge from the source parallel to one another, it is necessary to ensure accurate alignment of the apertures in the different grids. To ensure this, the grids for all the sources were drilled, and the support structure aligned, using a special jig and dowel arrangement.

As explained in 3.1 above, only one ion flux to the aperture gives a parallel beamlet for a given geometry. With this source, the plasma density varied by ∓ 15% over the area enclosing the extraction apertures, a diameter of 80 mm. This was compensated for by varying the accelerating gap to match the measured ion flux, achieved (to the required accuracy) by dishing the grids and using slightly different radii of curvature for the first and second grid. As can be seen from equation (3), the optimum current varies inversely as the square of the acceleration gap, hence a variation of 15% was sufficient to compensate for the 30% variation in plasma density.

The specified pulse length was 30 msec. The grids of an extraction system receive power not only from the backstreaming electrons mentioned in 3.4.1.2 above, but also directly from plasma impinging on the first grid. For this source, the temperature rise was shown to be tolerable with only edge cooling of the grids [8]. However, the grids did expand, and to ensure that all the grids moved in the same direction, the grids were dished towards the plasma source. Such a dishing obviously gives a mechanical focusing by directing all the beamlets towards the centreline. The radius of curvature of

the grids was chosen to optimise the beam transmission to the tokamak. The necessity to dish the grids was also convenient in matching the non uniform plasma to the extraction system (as already discussed). by using different radii of curvature on the plasma and decel grids.

The CLEO source was also used as the basis for the first neutral injectors installed on the DITE tokamak and for those used on the CLEO stellarator experiment, both at Culham Laboratory. For these experiments, the pulse length had to be extended to 100 msec. The introduction of water cooling to the grids would have greatly complicated the structure, and this was avoided by changing the grid material from copper to molybdenum. The main restraint on the pulse length arose from the need to avoid buckling of the grids by thermal expansion. Although the specific thermal capacity ($\rho * Cv$) of Mo is less than that for Cu, $2.5 * 10^6$ J/m^3 °C cf $3.6 * 10^6$ J/m^3 °C, this is more than compensated for by the lower coeficient of expansion, $5 * 10^{6}$/°C cf $16.6 * 10^{-6}$/°C. Thus for the same power input, Mo can be allowed to have three times the temperature rise for the same thermal expansion, just sufficient to allow the increase from 30 msec to 100 msec required.

3.4.1.3 Beam Species/Gas Efficiency/Beamlet Divergence

The electrons in the expanded plasma region were not easily lost at the walls as they were confined by the magnetic field, nor at the extraction grid as this was electrically floating, so that the total electron loss could only equal the ion loss to the grid. (Ion loss to the grid is relatively low as the ions are massive and move slowly compared to the electrons.) This meant that the ionising electrons had a relatively long path length in the source and they were efficiently used in ionising the H_2 gas. As a result, the CLEO source could operate at full performance with a gas efficiency of 50%, defined as the ratio of the number of nuclei leaving the source as fast ions to the number of nuclei introduced as H_2, with a minimum operating pressure of ~ 0.8 Pa. The pressure drop across the grids ensured a maximum pressure of ~ 0.5 Pa in the extraction system.

The species extracted from the CLEO source was determined by analysing the spectrum obtained from a magnetic momentum analyser sampling a small

fraction of the beam. The measured species in the extracted beam were 65:20:15 of H^+:H_2^+:H_3^+.

The divergence of the beamlets was deduced from the thermal footprint on a calorimeter situated at the focal point of the extracted beam. The power density in a beamlet has been found to be accurately described as

$$P = P_0 * \exp-(r/r_0)^2 \tag{5}$$

where P is the power density a distance r from the beamlet axis, P_0 is the power density at the beamlet axis, and r_0 is a constant. The beamlet divergence is normally defined as

$$\omega_0 = \tan^{-1}(r_0/z) \simeq r_0/z \tag{6}$$

where z is the distance from the aperture to the point at which r_0 is measured. With the CLEO source, ω_0 was measured as 28 milliradians.

3.4.2 Rectangular Sources

As the parameters of fusion plasmas improved, it was necessary to increase not only the energy of the neutral beam systems, but also the power delivered to the plasma, and a large increase in beam current was required. Clearly this could have been achieved by increasing the number of sources, but limitations on the number and size of access ports for the beams made this unrealistic on many machines. As severe difficulties were encountered in scaling the CLEO source to larger diameters, which would have allowed an increase in the area available for extraction apertures, a new type of source was needed. The shape was to be rectangular in order to allow a close packing of sources if more than one per injector was required, which turned out to be the case.

Developments at the Lawrence Berkeley Laboratory in the USA had led to a rectangular source giving a 70 A hydrogen beam from a source free from externally applied magnetic fields (the "Berkeley field free source") [9, 10]. Unfortunately this source suffered a number of deficiencies, amongst them low electrical and gas efficiencies, and a poor proton yield, all of which made it unattractive as a candidate for (then) future neutral beam systems.

A large rectangular version of the CLEO source was constructed, which was designed to illuminate an extraction area 80 * 360 mm^2. Although electrically very efficient, the uniformity over the intended extraction area was not within the requirements, and this was abandoned in favour of the two sources described below.

3.4.3 The Reflex Plasma Source

This source was developed at Culham Laboratory for use on the Wendelstein VII stellarator at the IPP laboratory, Garching bei München, Germany [11, 12]. The required extraction area (80 * 360 mm^2), current (30 A), voltage (30 kV) and pulse length (100 msec) were the same as those required for the DITE phase II source described below, and the source used the same extraction electrode support structure and insulators as that source. The extraction system differed from that of the DITE source in two significant ways. First the overall beam was focused to the very short focal length of only 1.5 m. Second, the apertures were larger and the extraction aperture was shaped to give a lower beamlet divergence.

As already discussed in 3.1, a correct plasma boundary is necessary if a "parallel" beamlet is to be produced. It is intuitively obvious that the boundary will follow the electrostatic potentials of the extraction field, and that these will, at least to some extent, be set by the shape of the aperture in the grid. It is also clear that a cylindrical hole in a finite thickness grid is unlikely to lead to a spherical equipotential at the plasma boundary either if the plasma stays attached to the aperture edge at the source side of the grid, or if it protrudes into the bore of the aperture. This means that at the edge of the aperture the plasma boundary is likely to be excessively curved and lead to the periphery of the beamlet being abberated. It can be shown that the ideal shape is a knife edge where the angle between the metal and the beamlet envelope is the so-called Pierce angle of 67.5°. Equipotentials of a cylindrical and a shaped aperture (in the absence of a beam and any space charge) are shown in Fig.5.

In its final form, the source superficially resembles the later versions of the Berkeley field free source mentioned above. The source consists essentially of a rectangular box structure made up of a backplate and side walls, part of which act as a peripheral anode. Electrical vacuum

feedthroughs for eight tungsten wire filaments were let through the backplate. The filaments used were those developed for the DITE source described below. The sixth side of the box was insulated from the side walls and carried the extraction electrodes. A large rectangular magnetic coil was situated behind the source with its axis parallel to the source axis. In operation, the filaments were directly heated and run temperature (or emission) limited, and the arc supply, typically 120 V, was connected between the common point (the negative leg) of the filaments and the anode. Electrons emitted by the filaments (primary electrons) were accelerated towards the anode, but were inhibited from reaching it by the externally imposed magnetic field. Also these electrons were prevented from reaching the walls and the extraction grid by biasing these ~ 30 V negative wrt the filaments. Thus the electrons were contained within the source, losing their energy by exciting or ionising the H_2 gas which was introduced around the edge of the backplate, until they were eventually lost at the walls.

The externally applied field was kept low, $< 2 * 10^{-3}$ Tesla, in order not to degrade the plasma uniformity, but nevertheless resulted in approximately a factor two improvement in the electrical efficiency compared with a field free version of the source, although the overall electrical efficiency was still low.

The good confinement of the primary electrons within the source resulted in effective usage of the filaments as they could be operated at reduced temperature, and their lifetime correspondingly increased. This efficient usage of the primary electrons also made for an increased gas efficiency and a greater tolerance in gas flow conditions, thus avoiding several of the problems associated with the Berkeley field free source.

The two main problems with this source were the relatively low proton yield and the difficulty of scaling to larger versions.

3.4.4 Bucket Sources

In the early 1970's, Limpaecher and his co-workers at UCLA were creating and studying large volume quiescent plasmas created inside a metallic vacuum enclosure [13]. Losses of ionising electrons and plasma at the walls were reduced by magnetic fields from permanent bar magents placed against the

outside of the walls. Various arrangements of magnets were used, one successful variant being lines of magnets all with one pole facing the wall, the polarity alternating from row to row, as sketched in Fig.6. With this arrangement, the multi-polarity of the magnet array means that the magnetic field decreases very rapidly with distance from the array. Thus a plasma created within a chamber using this confinement scheme would experience little magnetic field throughout the body of the plasma, but strong fields near the walls. Any ionising (primary) electrons (energy > 50 eV) would be well confined, and a strong plasma density gradient should only exist at the edge, in the region affected by the magnetic fields. The density gradient in the main volume of the plasma needs only to be sufficient to ensure that the diffusion of plasma from the centre equals that across the strong magnetic field at the walls, which necessitates a relatively shallow gradient. This idea seemed directly applicable to the needs of the plasma sources for beam extraction, replacing one wall with the extraction system. As this magnet arrangement suggests a sort of magnetic bucket, this name is commonly used in referring to the sources using this concept.

A small cylindrical source based on the above ideas was constructed at Culham in 1976. This was 150 mm in diameter, 150 mm in length. Lines of magnets of alternating polarity was arranged parallel to the axis of the cylinder, and each line was continued radially towards the centre of the backplate, as sketched in Fig.7a. An array of Langmuir probes took the place of an extraction system at the opposite end. Tantalum wire filaments were supported on electrical vacuum feedthroughs on the side wall. The permanent magnets were made from Cobalt Samarium in an epoxy binder. These had a relatively high surface field (~ 0.2 Tesla) and were easily machined to make the radial array for the source backplate. This source behaved essentially as indicated above. It was found that the field decayed rapidly with distance from the walls falling to ~ $2 * 10^{-3}$ Tesla in ~ 50 mm. Electrons were accelerated from the directly heated filaments towards the walls which were held at ~ 100 V positive w.r.t the filaments and a plasma was created by ionisation of H_2 fed through the backplate. This was found to be uniform within the $2 * 10^{-3}$ Tesla field contour (see Fig.7b), and plasma densities in excess of those needed for the ion acceleration systems of the beam sources were readily achieved.

3.4.4.1 The DITE Phase II Source

As a result of the success with the small cylindrical source described above, it was decided to embark on a full size version for the DITE phase II injectors in parallel with the reflex source described in section 3.4.3. This had to illuminate uniformly an extraction system 80 * 360 mm^2 with a current density of ~ 2 kA/m^2 to give the specified 30 A of beam current. As it fitted more naturally to the rectangular format, the lines of magnets were run orthogonal to the source axis, around the source walls. Decreasing rectangles of magnets completed the array over the source backplate. Filaments were mounted off vacuum feedthroughs on the backplate.

The filaments used for all previous sources at Culham had been made of 1.6 mm diameter Tantalum wire. This is an excellent material, but in use in an ion source the surface of the filaments became heavily pitted, leading to local reductions in diameter, hence increased heating at those points, leading to enhanced evaporation and a reduction in lifetime. Additionally Tantalum is soft at the normal operating temperatures, and easily sags under its own weight, which can cause an electrical short. For these two reasons alternative materials were sought. Only tungsten seemed a viable alternative, although in principle it appears worse than tantalum since at the temperature for the same thermionic emmission, the evaporation rate is higher for tungsten. Also it is more difficult to make filaments from tungsten as it is not easily workable even at high temperature. Nevertheless, it was decided to use simple hairpin filaments of 1.6 mm diameter tungsten wire for the DITE source, and this proved to be a great success, with no filaments being lost through melting or evaporation throughout the life of the sources, in excess of 100,000 arc and filament pulses of > 5 sec. The filaments were found to be almost unaffected by their life inside the ion sources, showing none of the deleterious surface pitting observed with the tantalum filaments. (Both silicated and thoriated tungsten were also tried, with no improvement over pure tungsten being observed. It is likely that the thorium or silicon are lost from the filament via the hydgrogen ion back bombardment.)

Initial operation of the DITE source was only partially successful as it was found that the source uniformity was much worse than predicted. The magnets had been arranged to give a low magnetic field throughout the source volume. Unfortunately, the volume field was checked using an uncalibrated

Gaussmeter, and later careful checks revealed that the (axial) magnetic field in the proposed plane of the extraction system was ~ 2 * 10^{-3} Tesla. This arose from the orientation of the magnet lines orthogonal to the source axis. With a finite array of this type a "super-cusp" is formed over and above the cusp field between adjacent lines of magnets. This is sketched in Fig.8a. The resultant axial field in the extraction plane caused the non uniformity of the plasma. To demonstrate this, a reverse axial field was applied externally using one of the coils from the reflex sources described above. If the external field added to the super cusp field, the uniformity deteriorated, if it substracted, the plasma could be made uniform. It is evident that as the axial field reverses at the super cusp, the field is zero in the plane of the super cusp. Thus it was decided to locate the extraction plane at the super cusp by making the extraction system slightly re-entrant into the plasma source. Subsequent measurements demonstrated that the plasma was indeed uniform across this plane. Although the orthogonal magnet array and subsequent super cusp were an initial disadvantage, it turned out that a significant advantage arose, as will be described below.

In this final form, the operational aspects of the source exceeded the requirements and expectations [15, 16] and are listed in the table below:

Characteristic	Achieved		Required
	Best	Operational	
Plasma densities	> 8 kA/m^2	2.5 kA/m^2	2.5 kA/m^2
Operating pressure	~ 0.05 Pa	0.5 Pa	< 0.5 Pa
Arc Voltage	35 V	90 V	< 120 V
Arc Current	> 500 A	300 A	< 600 A
Electrical efficiency	~ 7 A/kW	~ 1 A/kW	> 0.3 A/kW
Plasma uniformity	< ± 10%	< ± 10%	< ± 10%
Species mix (H^+:H_2^+:H_3^+)	81:9:5	75:15:5	>65% H^+
Extracted current	45 A	30 A	30 A

The parameters listed above under "best" were not all simultaneously achieved, but those listed under "operational" were. For example, in the above table, the electrical efficiency is taken as the ratio of the extracted beam current to the arc power and this was found to decrease linearly with the arc voltage over the range of interest [16]. The decrease in electrical efficiency was, however, not as rapid as the increase in arc voltage, and so lower arc current could be used at the higher arc voltages to reach the same extracted current. This meant that the temperature of the filaments could be decreased, reducing tungsten evaporation, and increasing filament lifetime. The optimum operating point was found to be at an arc voltage of ~ 90 V.

The source was found to be very easy to operate, being very tolerant of variations in the gas flow, or (small) arc voltage fluctuations. An unexpected bonus was that the measured species mix was gratifyingly high, ~ 75% H^+ at 2 kA/m^2. The underlying reason for this was not properly understood at the time, but was the consequence of the super cusp mentioned above. The effect is more fully described in the discussion of the JET source below.

The extraction system for the DITE phase II source was based on the experience gained with the CLEO source. The apertures and the grid spacing in the accelerator were identical to those of the CLEO source. The pulse length requirements were the same as those for the DITE phase I system, 100 msec, and it was decided to use inertially cooled grids based on the technology used for the CLEO source. As the total extraction area was to be increased by approximately a factor 4, it was decided to subdivide the extraction grid into 4, so that each sub grid would have dimensions similar to those of the CLEO source grids. Each sub grid was drilled over an area of 80 * 80 mm^2 with a hexagonal array of 431 holes. The sub grids were mounted side by side on a rectangular support box to form the required 80 * 360 mm^2 extraction area, and each grid was cooled between pulses by conduction to the support box.

In order to transmit the beam through the narrow DITE port, it was necessary to focus the beam to a distance of ~ 3 m. This was achieved by a combination of methods. First as with the CLEO source, the grids were dished

to give thermal stability, and provide some focusing. (The greater uniformity of this source meant that differential curvature of the extraction grids was unnecessary and the curvature was kept to the minimum for thermal stability.) Secondly offset apertures on a suppressor sub grid ensured an overall focus of 3 m for that sub grid assembly. Lastly, each sub grid was aimed towards a common point at 3 m by angling the appropriate part of the support box, ie. the end of the support box was machined to have 4 angles forming chords to a circle of 3 m radius. An artists impression of the final source is shown in Fig.8b.

3.4.4.2 The JET Source

At the end of 1979, a committee was set up with members from Culham laboratory, JET and the laboratory of the French CEA at Fontenay-aux-Roses, Paris (FAR) with the brief to design the neutral injectors for the JET project. These were to deliver 10 MW of neutral power at 80 keV/nucleon for pulse lengths of < 20 sec. The sources had to operate initially at 80 kV with H_2, with the cabability to be modified to operate to 160 kV with D_2.
It was decided that two injectors would be used to deliver the required 10 MW of power in the full energy component, ie. the neutral beam derived from the extracted atomic ions. The basic geometry of the JET port had already been decided, and this together with the length of the final system necessitated beamlet divergences of < 0.7°. As with the injectors already mentioned above, focusing of the beam would be necessary to transmit the beam through the port. Penetration of the large size of the anticipated high density and temperature of the JET plasma determined the need for 80 keV/nucleon beams. This also meant that the power in the fractional energy neutrals was assumed not to be useful for heating the plasma, and that a high power in this component of the beam would actually be deleterious. JET specified a minimum proton fraction of 80% in the extracted ion beam.

The final design for the JET injectors required 8 beam sources per injector, each delivering either 60 A of hydrogen beam at 80 kV, or 30 A of deuterium beam at 160 kV, for up to 20 secs. The maximum extraction area (set by geometric constraints on the beam transmission through the JET port) was $180 * 450\ mm^2$.

The proposed development of the JET injection system represented a large step in almost all parameters - 2 to 4 times the energy of any previous European ion source, with an extraction area ~ 4 times any previous source, and essentially dc operation, which required actively cooled grids, plasma source, beam dumps etc. Large gas flows result directly from the large extraction area with consequent massive pumping capacity requirements. As far as the source was concerned, the most important advances were seen as operation at 80 kV and then 160 kV, the development of a plasma source capable of illuminating the large extraction area that would be needed to obtain the 60 A beam, and actively cooled grids. It was therefore decided to develop the two types of plasma sources in use at FAR and Culham, the periplasmatron and the bucket respectively, and that both laboratories would test the 80 kV source. Both plasma sources were successfully developed [17, 18, 19], but only the development of the bucket, which is the source actually used on JET, is described here.

At the time of the JET source development, the reasons for the measured variation in proton yields from various sources was not well understood. A prevalent theory at that time related the proton yield to the volume of plasma in the source, and the first successful bucket source built to illuminate the JET extraction system was designed to maximise the plasma volume. The source used a "checker board" arrangement of the permanent magnets. This consisted of rows of magnets running around the rectangular source, each magnet being ~ 50 mm long, ~ 13 * 10 mm^2 cross section. Adjacent magnets had the opposite pole pointing towards the source wall and the magnets in adjacent rows had opposite polarities. Thus in the plane of the source walls and backplate, the magnet polarity alternated in two orthogonal axes, like the colours of a checker board. The very high polarity of this arrangement gave a very rapid fall of the magnetic field with distance from the source wall, hence a very large uniform plasma volume. Although this proved to be the case, the proton yield was disappointingly low at the operating plasma density, typically 65% at 2 kA/m^2.

A simple theory evolved from work in the USA [20] suggested the reason for this low proton yield, the reason for the high proton yield of the DITE phase II source, and also a way to improve the JET source. That work involved dividing a bucket source into two with a set of parallel rods containing permanent magnets. The idea was to set up a magnetic field across the source

which would act as a filter; the field would be sufficiently low that ions would easily pass through, slow (thermal) electrons would be sufficiently collisional that they would also easily cross the field, but fast (primary) electrons would be reflected. Thus if the filaments were located only on one side of the filter, primary electrons would only exist on that side of the filter. This region of the source is termed the driver region. On the other side of the filter there would be only low energy electrons, hence few ionising collisions, ions coming only from the other side of the filter. The extraction grid would form the end wall of this region, which is termed the extraction region.

The absence of primary electrons in the extraction region means that there is essentially no creation of H_2^+ there. Both H_2^+ and H_3^+ are destroyed by dissociative attachment ie.

$$e + H_2^+ \rightarrow H + H$$

and

$$e + H_3^+ \rightarrow H_2 + H$$

and both these reactions are fast for low electron energies. The only loss mechanisms for H^+ are wall recombination and recombination with H^-, both of which are also loss mechanisms for H_2^+ and H_3^+. Thus in the extraction region, the molecular ions are preferentially destroyed and not created, so that the fraction of protons is enhanced.

In the DITE phase II source, it was likely that the super cusp described above acted as this magnetic filter. Thus the way to improve the proton yield of the JET bucket source seemed to be to create a super cusp. Many configurations of permanent magnets were tried, and the species yields measured, confirming the theory outlined above. The final magnet configuration chosen gave both a high proton yield, exceeding the specified 80% at 2 kA/m^2, and a good plasma uniformity across the extraction grids. The measured species yield is shown for both H_2 and D_2 operation in Fig.9 [21].

A significant increase in source size compared to previous sources was needed to illuminate the large extraction area, which necessitated a proportional increase in the arc current. To provide this increase, the design allowed for 24 filaments similar to those used on the DITE phase II source. One important innovative decision for the JET source was to heat these with ac instead of dc current, as had previously been the case. Combined with a transformer located at the back of the source, this enabled a simple 3 core lead to transmit the filament power from supply to source, a distance of 50 - 100 m, cf 48 high current (~ 100 A) leads. An additional bonus is the increase in filament lifetime. As the arc current flows from the filaments to the negative of the arc supply, in the case of dc heating of the filaments, this adds to the heating current in one leg of the filament and subtracts in the other. This leads to assymmetric heating and thus assymmetric electron emission and filament evaporation. The end result is that one leg burns out first. With ac heated filaments the assymmetry is time averaged over the whole filament. The results to date from JET indicate a uniform loss of material and a considerably extended filament life.

At the time of this development, no three grid system of the type described in 3.1 above had been operated at above 50 kV, and it was believed that equation 3 was valid. Therefore it was decided that in order to obtain the specified beam current density for the 80 kV JET source a four grid accelerating stack was required. The design and single aperture experimental verification of the beam optics were carried out by Culham laboratory.

The long, > 10 sec, pulse length required meant that actively cooled grids had to be developed. Measurements on prototype sources indicated that ~ 1% of the extracted beam power would be collected by the grids. Given operation at 80 kV, 60 A, this is ~ 48 kW. The extraction grid also receives power directly from the arc, and thus had to handle up to 75 kW. Given that the thickness of the grids has to be minimised (particularly of the gradient grid) in order to simultaneously keep the optimum current density high and to have good beamlet optics the cooling channels were to be 1 mm * 1 mm cross section, with one channel crossing a grid between each row of holes. The staggering of the apertures, necessary to pack sufficient apertures into the available area, meant that the channels had to be serpentine. Several methods of manufacturing such a grid were investigated, with electrodeposition being the most successful [22]. For this a baseplate is machined from pure copper

including the cooling channels. The cooling channels are then filled with conducting wax, then copper electrodeposited over the entire surface to the required thickness. The resultant grid is then heated to melt the wax, which can then be readily drained away.

As the JET source had to use materials compatible with both good vacuum practice and the expected neutron flux from the JET machine, it was decided that the use of organic materials should be avoided. Traditionally, epoxy had been used (CLEO, DITE etc) to form the main high voltage insulator, which acted as both vacuum wall and included the support for the grid holders, which have to be accurately positioned. For the JET source this had to be replaced by a ceramic material. The final solution uses a large cylindrical procelain insulator, to form the vacuum wall, with the grid holder boxes supported from a single flange at the high voltage end by precision high density alumina post insulators. The high voltage flange is sealed into the porcelain using a metal "helicoflex" seal (a kind of metal O-ring) to form the vacuum seal between a ledge ground into the procelain and the metal flange. A radiation resistant rubber O-ring outside the helicoflex creates a secondary vacuum barrier. The same technique is used to seal another metal flange to the other end of the procelain, which is held at ground potential. Intermediate potentials are fed to the appropriate electrodes through standard ceramic to metal vacuum feedthroughs on either the high voltage (gradient grid) or ground potential (suppressor grid) flange. All other seals, such as between the plasma source and the high voltage flange, are all designed for helicoflex seals, although normal Viton O-rings are presently being used. The JET source exhibits negligible degradation of performance when stored for long periods under vacuum, which is contrary to the experience with previous generation of ion beam sources, and this is attributed to the lack of organic materials in the sources.

The final source, given the name PINI from Positive Ion Neutral Injector, was tested at both Culham and FAR. Reliable long pulse operation was achieved at full parameters, 80 kV, 60 A at both laboratories. However it was found that the beam focusing was not as required. The extraction grid was made up of two halves inclined towards each other, whilst offset apertures steered each beamlet to give the required beam focusing. Experiments revealed that the offset aperture steering was a factor two stronger than predicted. This was shown initially with the help of the neutral injection group at the

Japanese Atomic Energy Resarch Institute with their three dimensional code, and later by detailed study with a similar 3D code developed by GSI at Darnstadt in Germany to be a three dimensional effect, not detectable with the 2D computer code that had been used originally to study the optics. Fortunately this was easily corrected by offsetting the apertures of the production sources less. The final grid system was shown to have the beamlet divergence (0.7°) and focusing required by JET.

At the same time as Culham were studying the JET 4 grid optics, FAR continued work on a 3 grid version, and eventually succeeded in demonstrating that equation 3 is not valid at high voltages. They proceeded to develop a 3 grid version of the JET 80 kV extraction system, which was shown to have very similar beam quality to the 4 grid version [23, 24]. Encouraged by this success, FAR proposed a 3 grid extraction system for the upgrade of the JET sources to 160 kV, D_2 operation. The proposed 3 grid upgrade needed only one new grid and an increase in the extraction gap, which had been allowed for in the design of the accelerator stack. The prototype, tested at FAR, demonstrated that the system was viable, with the requisite beam optics [25], and it has been adopted, and is now successfully in use on JET. A schematic cut away view of a JET source is shown as Fig.10. Fig.11 is a schematic of the extraction system showing the two configurations - for 80 kV and 160 kV operation.

3.4.4.3 The TEXTOR and ASDEX Sources

The success of the JET source led to derivatives being used as the basis of the neutral injectors for the TEXTOR and ASDEX upgrade tokamaks. The requirements of these systems were similar, 50 kV, 85 A in H_2, with the capability to operate in D_2 for ASDEX. The large current could be achieved by increasing the extraction area by simply enlarging the grids and using a 3 grid extraction system, based on the work at FAR carried out for JET. However, this meant illuminating a larger area, which was not possible with the high proton yield source, but the early checkerboard version described above was uniform out to the necessary dimensions. Thus only minimal changes were necessary to create a successful source. At the time of writing, the TEXTOR system is operational [26] and the ASDEX injectors are due to come into operation in 1991, all the sources having been tested.

4. Negative Ion Sources

The main driver in the development of sources based on negative ions has been the higher probability of conversion of D^- ions to D° which is ~60% for passage through a gas cell and this fraction is independent of beam energy up to the level required for future tokamaks. Thus negative ion sources are vital for neutral beam injectors for next step tokamaks. The reason for this high conversion probability is the very low binding energy of the additional electron for D^- and H^- (0.75 eV). However the corollary of this effect is that it is difficult to form the negative ion in the first place. It is the search for solutions to this problem which has been the basis for the research in this area.

There are additional problems which have to be solved; electrons are also negatively charged and the plasma source must suppress extraction of these particles without impairing the collimation of the H^-/D^- beam and additionally there is a new requirement for a degree of beam energy variation at fixed beam currents.

4.1 Negative Ion Formation Techniques

In many respects the requirements of the ideal negative ion source are very similar to those listed in section 3.3. Within the UK, the negative ion source development programme has followed an approach based on H^- production within the plasma volume by dissociative attachment to vibrationally excited H_2 molecules. Such sources are commonly known as "volume" sources as nearly all process occur in the plasma volume. The dominant vibrational molecule production reaction is:

$$H_2(\nu) + e^-(\varepsilon < 2eV) \rightarrow H^- + H$$

where ν is the vibrational quantum number and ε is the electron energy. The vibrational molecules themselves are also formed within the plasma volume and dominant channels of formation are:

$$e^-(\varepsilon > 20eV) + H_2 \rightarrow H_2(\nu) + e^-$$
$$H_2^+/H_3^+ + \text{wall} \rightarrow H_2(\nu) + \text{wall}$$

where "wall" signifies particle collision with the walls of the plasma chamber.

This method avoids the use of cesium as a catalyst (this is commonly used elsewhere) and yields a large area of plasma containing a modest density of H^- or D^- ions. This is very similar to the production of positive ions in the sources described earlier except for the lower current density of negative ions. The extraction of a high current of negative ions from the plasma has to make use of a large number of extraction apertures each one of which extracts a current given by equation (2):

There is an upper bound to the aperture radius to extraction gap ratio, a/d, of about 0.5 before aberrations dominate the beam divergence but the extraction potential is usually very much smaller than the final beam energy as the accelerator has more than one acceleration gap.

In Fig.12 is shown a illustration of a source with a single aperture (for simplicity) which indicates the plasma chamber where the negative ions are formed and a two gap accelerator which can accelerate a beam up to typically 100keV. Higher beam energies would need further gaps. The plasma source is of the magnetic multipole type described in section 3.4.4 but in this case it is modified to create a weak (B~ 50 gauss) field across the chamber as shown in Fig.12. This creates the correct conditions for ionisation and vibrational molecule production adjacent to the filaments where hot electrons exist whose temperature is typically 20-30eV.

However on the other side of the sheet field the plasma is much colder because of the much higher diffusion rate of cold electrons relative to hot electrons. If the field has the correct strength then the temperature falls below 2eV and dissociative attachment of these electrons to vibrational molecules occurs forming H^- ions. This low electron temperature also inhibits destruction of H^- by electron impact which sets in at temperatures in excess of 3eV. In many respects this field acts in the same role as the supercusp field described earlier for proton enhancement.

In the following sections we discuss in greater detail the formation of an H^- beam from the type of source shown in Fig.12.

4.1.1 Gas Density

The gas density, N, enters the formation process via the creation of vibrationally excited molecules as well as the formation of the positive ion-electron plasma by ionisation. However, if the plasma has good confinement of fast ionising electrons (see section 3.4.4) then it can be shown (Green et al [27]) that:

$$\frac{1}{j_{-0}} = \frac{A}{j_{+}} + \frac{B}{N} \qquad (7)$$

where A is a dimensionless constant of order unity and B is a function of the rate processes which lead to H^- formation. The term j_+ is the positive ion current density (usually relatively independent of pressure) and j_{-0} is the negative ion current density leaving the plasma.

The above expression is unusual in that it indicates that for a given pressure there is an absolute maximum value of j_{-0} that can be produced, even if the arc current in the discharge (and hence j_+) tends to infinite values. Alternatively for a given j_+ value, there is also an upper limit to j_{-0} even if the pressure becomes very high.

It is this latter effect which causes some problems as there is also loss of H^- or D^- ions during extraction by collision with the background gas exhaust from the source within the accelerator. This gives an exponential attenuation of the beam according to the expression:

$$j_- = j_{-0} \exp\left(-\int N \sigma_{-0} \, dz\right)$$

$$\simeq j_{-0} \exp\left(-\alpha \, d \, N \, \sigma_{-0}\right) \qquad (8)$$

where α is a dimensionless constant of order unity. The factor α arises from the fact that the pressure profile along the accelerator axis decreases approximately linearly with distance from the plasma boundary.

Thus combining the two expressions gives:

$$j_- \simeq \left(\frac{N j_+}{AN + B j_+} \right) \exp(-\alpha d N \sigma_{-0}) \qquad (9)$$

There is an optimum value of N for which j_- is maximum and this optimum is a function of j_+ and d for fixed values of the rate coefficients. In general the value of N for maximum j_- increases for rising values of j_+ (or arc current) and also for decreasing values of the aperture radius as a/d is typically in the range of 0.3 to 0.6.

4.1.2 Beam Collimation

Contrary to expectation, beam collimation in these dissociative attachment sources is quite different to the analogous positive ion bucket sources. A generic two gap acceleration system is shown in Fig.12. Focusing is achieved when the ratio of the potentials across each of the first and second gaps is 1:6, and this ratio is nearly independent of beam current [28]. This behaviour is different from positive ion systems and is more analogous to electron guns with rigid cathodes. This effect may be caused by the magnetic field across the extraction aperture used to suppress electrons which can stiffen the plasma surface against the electric field pressure.

There is however an upper limit to the current that can be transported through the accelerator which given by equation (2) and this is further attenuated by stripping losses as indicated in equation (9). Thus a small value for d (and hence a) is preferable and as large a value as possible for V_1, the first gap potential. It will be seen later that electron suppression and trapping limit the range of values for V_1.

The independence of beam collimation on the beam current weakens considerably the need for a highly uniform negative ion current density. Each beamlet will be focused when the correct voltage ratio is achieved and the current is simply what the plasma supplies to that aperture, subject to an upper limit. A uniform beam is still desirable as it influences the power deposition within tokamak, and, for a given current, this limits the maximum power deposited on the residual ion dumps. Additionally the beam power deposition is more easily predicted for a uniform source and eases the beam steering and manipulation problem. Also significant density gradients across

the extraction apertures can lead to beam steering (off axis deflection) and aberrations which can cause loss of beam in the injector or in the duct to the tokamak.

The beam energy for negative ion injectors will require more than two gaps to accelerate the beam. Code calculations show that the voltage ratio above applies to the first two gaps only and the following gap potentials are almost a free choice as the space charge of the negative ion beam from these sources is very weak and the beam is essentially collimated by the first two gaps. This makes beam energy variation very straightforward as the extraction is controlled by the first two (or possibly three) gaps and the downstream gap potentials can be readily adjusted without altering the optical quality of beam. Calculations show that over a factor of two change in energy is obtainable. This is shown in Fig.13 which is the output of the ion-ray tracing code Culham-AXCEL.

4.1.3 Electron Suppression

The fractional density of negative ions rarely exceeds 0.5 of all negative charge in the electrically neutral plasma, the remainder being electrons. Application of a positive potential would hence also extract electrons as well as negative ions and the high velocity of electrons (due to their low mass) compared with negative ions would lead to the beam current comprising almost totally of electrons. This would negate the high conversion efficiency of D^- conversion to D° as the injector input power would be expended in electron acceleration.

In ion sources developed in the UK, this is prevented by application of a magnetic field across the extraction aperture which is strong enough to prevent diffusion of cold electrons. The field lines intersect positively biassed collection areas so that electrons gyrating round these field lines are progressively removed. A model of this has been developed which yields the simple expression (Haas and Holmes [29]:

$$I_e = I_{eo} \exp(-\beta B d \exp(-\varphi/T_e)/T_e^{1/2}) \quad (10)$$

where B is the field, d is its depth, T_e is the electron temperature and β is a constant. The advantage of a high field is obvious subject to the limit of not deflecting the H^- or D^- beam itself noticeably.

In the absence of any electron suppression, I_e/I^- is typically 60 for hydrogen and 100 for deuterium. With a practical suppression system, experimental values of I_e/I^- as low as 0.5 have been obtained in hydrogen and 2 in deuterium using a field-depth product of 0.25 T.mm. Higher fields start to give problems with transport of the negative ion beam.

4.1.5 Electron Trapping

Even the low fractional currents described above would still reduce the injector efficiency drastically in addition to being an intense source of x-rays if the electrons were accelerated to high energies. This would lead to further secondary electron emission and electrical breakdown within the accelerator. To avoid these problems, it is essential to trap the electrons at a low fraction of the final energy. This can be achieved by adding further magnetic fields within the accelerator as shown in Fig.14 which are used to deflect the electrons out of the beam path.

The lowest dump energy of the electrons is the potential across the first gap of the accelerator. Bar magnets placed at the upstream face of the second electrode deflect the electrons by about 90° onto collecting surfaces within the electrode. The focusing requirement described in section 4.1.3 indicates this potential has a maximum value of 0.14 of the beam energy for a two gap accelerator and could be much smaller for higher energies. This is described in greater detail in section 4.3.

However a magnetic field within the accelerator does deflect the D^- (or H^-) beam by 1/68 (1/43) of the electron deflection, typically 1.5 to 2°. This is corrected by adding further magnets in the downstream face of the second electrode and in subsequent electrodes which restore the negative ion beam to the geometrical axis of the accelerator. These fields also have the effect of removing further electrons from the beam which are created by further stripping of the negative ions or by secondary electron emission from the electron dump in the second or subsequent electrodes.

4.1.6 Particle Extraction from the Beam Plasma

It might be thought that negative ion beam accelerators have a reverse positive ion beam similar to the electron problem discussed in section 3.2. However such a reverse ion beam is only just detectable in experiments with negative ion accelerators and appears to have no discernable effect on the negative ion beam. Experiments with an extra suppression electrode show no change in negative ion beam divergence or in total beam current when the positive ions are suppressed. In present and future designs of accelerator structures, use of this electrode has now been abandoned.

The reason for this fortunate difference compared with positive ion accelerators is straightforward. Firstly, the production rate of slow positive ions by negative ion beams is smaller than ionisation and charge exchange by positive ion beams and the beam current density itself is typically 10% of a positive ion beam. Secondly magnetic fields at the last acceleration electrode (which are used for the beam alignment as described above) are supplemented by magnets at the neutraliser entrance (if present), and these keep the beam plasma away from the aperture. The combination of these two effects leads to a very low current of positive ions being extracted from the beam plasma.

The positive ions in the beam plasma downstream of the accelerator are trapped by the beam and ensure that the point where the negative ion beam becomes space charge neutralised is close to the ground (last) electrode of the accelerator column, hence preventing beam divergence problems.

4.2 Negative Ion Source Development in the UK

4.2.1 The First Prototype

The first true negative ion source in the UK was built at Culham Laboratory in 1982 [30]. It was a magnetic multipole source built according to the concepts proposed by Bacal [31] and produced negative ions following the processes outlined above. A schematic drawing of the source which is shown in Fig.15, this was built for pilot experiments into the production and extraction of single aperture beams from the plasma volume. At this early

stage it was too premature to propose building an injector from sources of this type.

The plasma source shown in Fig.15 was essentially a stainless steel box 200 x 240 mm^2 in area and 200 mm deep with two hot wire tungsten cathode filaments and the box, which formed the anode, was lined on the outside with Co-Sa bar magnets yielding a plasma face cusp field of 0.15 T. The accelerator was a three electrode structure of the type shown in Fig.12 where the basic principles of negative acceleration could be tested. The main source filter field was created by pattern of magnets on the longer source sidewalls, and the electron suppression field by two smaller bar magnets on either side of the beam forming aperture in the first grid which forms the sixth side of the plasma source. This electrode was biassed positively with respect to the anode by a few volts in order to collect the electrons which were trapped on the suppression field lines.

The basic performance of this source in hydrogen is shown in Fig.16 as a function of arc current and gas pressure. As expected a clear saturation with rising arc current is seen, which is in accordance with equation (7) as the positive ion current density is always linearly proportional to arc current. Higher negative ion current densities are obtained for larger gas pressures in the source but there is a strong indication of an upper limit, again in agreement with the model.

Beam focusing is obtained for a voltage ratio of $V_b/V_1 \simeq 6$ and a typical beam profile is shown in Fig.17. (V_b is the second grid voltage). As can be seen, the beam profile has a very similar gaussian half-width (ie. at 0.37 of peak intensity) to the extraction aperture radius even after a drift distance of 1.1 metres. This very low divergence indicates that the beam has a very low (if not zero) effective space charge because of the presence of slow positive ions (and some electrons) in the beam channel. Positive ion beams at beam energies of 40 keV are considerably more divergent as seen in section 3, mainly due to the fact that electrons do not compensate for the positive ion beam space charge so effectively due to their higher mobility.

4.2.2 The Negative Ion "PINI" Source

It was realised in 1984 that the prototype source was far too small for fusion applications and a much larger source needed to be developed. The earlier work on proton enhancement had shown that it was possible to incorporate a magnetic filter into the JET PINI and it would only be necessary to increase the strength of this field slightly turn this source in a generator of negative ions.

The first results from this (Holmes et al [32]) were very encouraging and are shown in Fig.18. A peak yield of 570 A/m^2 of H^- in the source was observed at discharge power of 140 kW with a 1.5 Pa filling pressure. In deuterium the performance is less good with a maximum of 250 A/m^2. Both of the above results were obtained with a small 10 kV accelerator with an aperture of 1.5 mm after correction of stripping losses during extraction. The data in Fig.18 is a reasonable fit to equation (7) showing that the model is in agreement with experiment.

The test facility for this source was also equipped with a battery of Langmuir probes which indicated that the plasma contained a substantial fraction of negative ions and had an electron temperature below 1 eV. The density of these negative ions obeyed the relationship:

$$H_2(v) + e \rightarrow H^- + H$$
$$H^- + H^+ \rightarrow 2H$$

so that: $$n_+ n_- = \alpha N^* n_e$$

where N^* is the density of vibrational molecules and α is a dimensionless ratio of rate coefficients. As N^* is a constant for fixed arc current and n_e is varied by altering the plasma grid bias, the product $n_+ n_-$ measured by the probe can be plotted against n_e and the result is shown in Fig.19 where a straight line is obtained in agreement with the equation above. The probes also revealed that a dipole filter created a non-uniform plasma arising from an E x B drift within the plasma which was orthogonal to the beam axis and the magnetic field. This non-uniformity was not a serious consequence for the large single aperture experiments but would be a difficulty for multiple aperture beams.

Up to this point only a limited amount of high energy beam extraction had been made, mainly on the prototype source described in section 4.2.1. This was remedied in 1986 by the construction of ISTS (Ion Source Test Stand) which could operate up to potentials of 100 kV and had a full range of beam diagnostics. This system was designed for d.c. operation with single apertures and aimed at supporting work in the area of the Strategic Defence Initiative although a significant part of the experiments were also of direct application to neutral beam injectors.

By the beginning of 1987 a peak current in excess of 130 mA had been extracted from a single 24 mm aperture with an electron current of 700 mA which was collected by the second electrode of the accelerator at an energy of 14 keV. However it was observed that the beam divergence was high and there was a substantial beam halo whose divergence was significantly in excess of 1°. This was improved by reducing the value of a/d from its initial value of 1.1 as shown in Fig.20 where the halo fraction is seen to be linearly proportional to a/d.

However there is a price to be paid for reducing a/d as can be seen from equation 2. The beam current decreased significantly and the best compromise was a value of a/d about 0.47 where a beam current of about 70 mA was achieved at a beam energy of 90 keV. At the same time a narrow core divergence of 3 millirads was obtained containing about 80% of the beam power. This represents a increase in central power density of about 50% compared with the earlier 130 mA result.

4.2.4 Deuterium Operation and Electron Suppression

Unlike positive ion sources, volume production of negative ions shows a strong isotope effect leading to a low D^- current density and higher electron current. Early operation with the large PINI negative ion source resulted in 250 A/m^2 D^- beam current density being produced in a non-uniform plasma as described in section 4.2.2. This non-uniformity was essentially eliminated by replacing the filter by a supercusp filter which is about a factor two stronger than that used for the proton enhancement experiments described earlier.

Optimisation of the supercusp strength and position yielded an increase in D^- yield up to a peak of 420 A/m^2 at a source pressure of 2.8 Pa. However in full scale operation with a long accelerator column a significantly lower operating pressure will be required to avoid stripping losses with consequent lower D^- yield. At the same time the electron current would increase as higher arc currents would be needed to give the required D^- yield as shown by equation (7).

Experiments on electron suppression confirmed the theoretical result described in section 4.1.4 and this is shown in Fig.21 for deuterium. The slope of the straight line agrees within a factor of two with equation 4.4 when the field is varied and the lower limit indicates that extracted electron currents below the D^- current are possible when the magnetic flux is in excess of 0.2 Tesla.mm. In this particular experiment a magnetic coil was used to create the magnetic flux but this would be difficult to extend to a multiple aperture array. Experiments with small bar magnets to replace the coil as shown in Fig.22 yield very similar levels of suppression providing the magnetic flux in the plasma is the same.

4.2.5 Future Injectors

As yet no neutral beam injector based on negative ions has yet been built but there is a plasma source and multiple aperture accelerator operating at 50 keV in pure hydrogen which has been tested in Japan [33] and also with a cesiated hydrogen discharge (Kojima et al [34]). This has shown that multiple aperture systems are possible, similar to those discussed above, with beam currents up to 3.4 A in pure hydrogen and 10.1 A for cesiated hydrogen discharge sources. In the UK there has been a considerable effort invested in the conceptual design of a neutral beam injector for NET and ITER which would operate at 1.3 MeV. A elevation view of the system is shown in Fig.23 where three injector modules are mounted in a vertical row to deliver 25 MW of neutral beam power through a single port of 3.4 x 0.8 m^2.

A more detailed view is shown in Fig.24 where two plasma sources, accelerators and neutralisers are mounted side by side in a single tank. Unlike all previous systems described in this paper, the plasma source is at ground potential. This approach gives the major advantage that virtually all the low voltage systems are also at ground potential making control interfaces

easy and eliminating the need for a high voltage platform which, at 1.3 MV, would be massive (> 100 m^3).

The plasma source is larger than the PINI by a factor of 4 in area and the accelerator is similar to Fig.12 for the first two gaps but then has additional electrodes at 220 kV intervals. These electrodes are resistively connected to a series of shields which surround the high voltage neutraliser and residual ion beam dump whose functions is to subdivide the gap between the neutraliser and earth planes.

This approach to the accelerator design also allows a variable beam energy as the voltage across the downstream 220 kV gaps can be reduced by a factor of two without significantly altering the beam focus. This permits a continuously adjustable beam energy from 500 keV to 1.3 MeV subject to the limits of the high voltage supply.

An additional requirement for the NET/ITER injectors is beam steering and profile control in one plane so as to be able to vary the profile of the driven current within the tokamak. This can be achieved by steering the beam by a series of electrostatic plates so that the beam can be simply deflected (equal voltage across gap) or focused and steered (unequal voltages across each gap). A similar but simpler system is used in the orthorgonal plane to separate the un-neutralised residual ions of D^+ and D^- from the D° beam just prior to the beam dump.

4.2.6 The Prototype D^- Injector, DRAGON

Many new ideas are included in the conceptual design of the injector for NET/ITER. Most of these are plausible and have been tested individually in earlier positive or negative ion systems but not together in a single injector unit. As part of a wider European programme for negative ion injector development it was decided in 1989 to build a prototype neutral beam injector which operate with a D^- beam. This experiment, called DRAGON, is sited at Culham Laboratory and is now in an advanced stage of manufacture.

The injector has most of the features required for the full scale system, including a grounded plasma source. The basic specification is for a 200 keV,

4 A beam of D^- ions (2.4 A of D^0 atoms). The system will operate for 2 seconds using a mixture of inertial and interpulse water cooling. A drawing of the side view of the injector is shown in Fig.25. The 200 keV accelerator follows exactly the plan for the 1.3 MeV accelerator up to the 200 kV electrode, the only difference being that the number of apertures is only 60% of the full scale system for one of the two plasma sources.

The plasma generator where the D^- ions are made has the same width and depth of the full scale unit but is only 2/3 the length as shown in Fig.26. This is an essential full scale test of the key features of the source including the magnetic filters, electron suppression and gas exhaust.

The neutraliser, electrostatic deflector and beam dump follow exactly the design principle of the full scale system but on a slightly smaller scale.

Active beam steering in this experiment of up to 10 milliradians is acheived by a magnetic field created by passing a high current (up to 1500 A) through the plasma grid. This field also forms part of the electron suppression field also forms part of the electron suppression system.

5. Conclusions

Over the past eighteen years, the development of intense ion sources for neutral beam injectors has advanced from the early 30 millisecond low voltage systems for CLEO to very sophisticated systems based on negative ions for the next step tokamaks such as NET or ITER. This progress has been based on a keen insight into the physical processes underlying the creation of these intense beams of positive or negative ions as well as the advanced engineering needed to turn these concepts into reality. As a result the Culham Laboratory and JET together with the CEA at Cadarache (formerly at Fontenay-aux-Roses) in France as part of a international collaboration around the world have demonstrated that neutral beams are an extremely successful method of injecting high powers into tokamaks to obtain thermonuclear ignition in a plasma.

References

1. Green, T.S., Reports on Progress in Physics, 1974, 37, 1257 - 1344.

2. Allison, S.K. and Garcia-Munoz, M, Chapter 19 of Atomic and Molecular Processes edited by Bates D R, Academic Press, New York and London, 1962.

3. Coupland, J.C., Green, T.S., Hammond, D.P., and Riviere, A.C., Rev. Sci. Inst., 1973, 44, 1258 - 1270.

4. Thompson, E, Proceedings of the Second Symposium on Ion Sources and Formation of Ion Beams, Berkley, USA, 1974, p.II.3.1 - II.3.5, and II.7.1 - II.7.4.5. Aldcroft, D.A., Burcham, J.N., Cowlin, M, and Sheffield, J, Nuclear Fusion, 1973, 13, 393 - 400.

5. Holmes, A.J.T., Phys. Rev. A, 1979, 19, 389 - 407.

6. Aldcroft, D.A., Burcham, J.N., Cole, H.C., Cowlin, M, and Sheffield, J, Nuclear Fusion, 1973, 13, 393 - 400.

7. Aldcroft, D.A., Burcham, J.N., Cole, H.C., Cowlin, M, Hemsworth, R.S., Sheffield, J, and Speth, E, Journal of Physics E, 1976, 9, 102 - 105.

8. Cole, H.C., Hammond, D.P., Jones, E.M., Riviere, A.C., and Sheffield, J, Rev. Sci. Instrum., 1973, 44, 1024 - 1028.

9. Berkner, K.H., Baker, W.R., Cooper, W.S., Ehlers, K.W., Kunkel, K.W., Pyle, R.V., and Stearns, J.W., Proceedings of the Second Symposium on Ion Sources and Formation of Ion Beams, Berkley, USA, 1974, I.5.1 - I.5.5.

10. Ehlers, K.W., Proceedings of the 7th Symposium on Engineering Problems of Fusion Research, Knoxville, USA, 1977, 291 - 294.

11. Feist, J.H., Kolos, J, Ott, W, and Speth, E, Proceedings of the 7th Symposium on Engineering Problems of Fusion Research, Knoxville, USA, 1977, 527 - 529.

12. IPP Neutral Injection Team, 8th Symposium on Engineering Problems of Fusion Research, San Francisco, 1979, 964 - 966.

13. Limpaecher, R, Mackenzie, K.R., Rev. Sci. Instrum., 1973, 44, 726 - 731.

14. Leung, K.N., Hershowitz, N, and Mackenzie, K.R., Phys. of Fluids, 1976, 19, 1045 - 1053.

15. Hemsworth, R.S., Aldcroft, D.A., Allen, T.K., Burcham, J.N., Cole, H.C., Cowlin, M, Coultas, J, and McKay, W, Proceedings of the Joint Varenna-Grenoble International Symposium on Heating in Toroidal Plasmas, Grenoble, France, 1978.

16. Hemsworth, R.S., Stork, D, and Cole, H.C., 9th European Conference on Controlled Fusion and Plasma Physics, 1979.

17. Duesing, G, Altmann, H, Falter, H.D., Goede, A, Haange, R, Hemsworth, R.S., Kupshus, P, Stork, D, and Thompson, E, 1987, Fusion Technology, 11, 1, 163 - 202.

18. Culham Neutral Beam Development Group Proceedings of the 13th Symposium on Fusion Technology, Varese, Italy, 1984, 693 - 702.

19. Becherer, R, Fumelli, M, and Valckx, F.P.G., Proceedings of the 7th Symposium on Engineering Problems of Fusion Research, Knoxville, USA, 1977, 287 - 294.

20. Ehlers, K.W., and Leung, K.N., Rev. Sci. Instrum., 1982, 52, 1452 -1456.

21. Deschamps, G.H., Falter, H.D., Hemsworth, R.S., and Massmann, P, Proceedings of the 15th Symposium on Fusion Technology, Utrecht, Holland, 1988, 588 - 592.

22. Altmann, H, Proc. 13th Symp. on Fusion Technology, Varese, Italy, 1984, 579 - 585.

23. Fumelli, M, Bariaud, A, Becherer, R, Desmons, M, Raimbault, Ph, and Valckx, F.P.G., Proceedings of the 3rd Neutral Beam Heating Workshop, Gatlinburg, USA, 1981, 549 - 558.

24. Raimbault, Ph, Fumelli, M, and Becherer, R, Proceedings of the 2nd Joint Grenoble - Varenna International Symposium on Heating in Toroidal Plasmas, Varenna, Italy, 1980, 935 - 944.

25. Fumelli, M, Bayetti, P, Becherer, R, Bottiglioni, F, Desmons, M, Raimbault, Ph, and Valckx, F.P.G., Proceedings of the 13th Symposium on Fusion Technology, Varese, Italy, 1984, 693 - 702.

26. Lochter, M, Private communication.

27. Green, T.S., Holmes, A.J.T., and Nightingale, M.P.S., Proc. 4th Symp. on Production and Neutralisation of Negative Ions and Beams, Brookhaven, USA, 1986, 208 - 218.

28. Holmes, A.J.T., and Nightingale, M.P.S., Rev. Sci. Instrum., 1986, 57, 2402 - 2408.

29. Haas, F and Holmes, A.J.T., 1990, submitted to J. Plas. Phys.

30. Holmes, A.J.T., Green, T.S., Inman, I, and Walker, A.R., Proc. 3rd Symp. on Heating in Toroidal Plasmas, Grenoble, France, 1982, 95 - 102, EUR 7979 EN, Commission of European Communities.

31. Bacal, M, Nicolopoulou, E, and Doucet, H.J., J. Phys. (Paris), 1977, 38, 1399 - 1406.

32. Holmes, A.J.T., Lea, L.M., Newman, A.F., and Nightingale, M.P.S., Rev. Sci. Instrum., 1987, 58, 223 - 234.

33. Watanake, E, Araki, M, Hanada, Moriike, H, Inoue, T, Kuravkima, T, Matsuada, S, Matsuda, Y, Ohara, Y, Okumura, Y, and Tanaka, S, Proc. 12th Symp. on Fusion Engineering, Monteray, Ca., 1987, paper 10-80.

34. Kojima, H, Hanada, M, Inoue, T, Matsuda, Y, Ohara, Y, Okumura, Y, Oohara, H, Seki, M, and Watanabe, K, Proc. 13th Symp. on Ion Sources and Ion-assisted Technology, Tokyo, 1990.

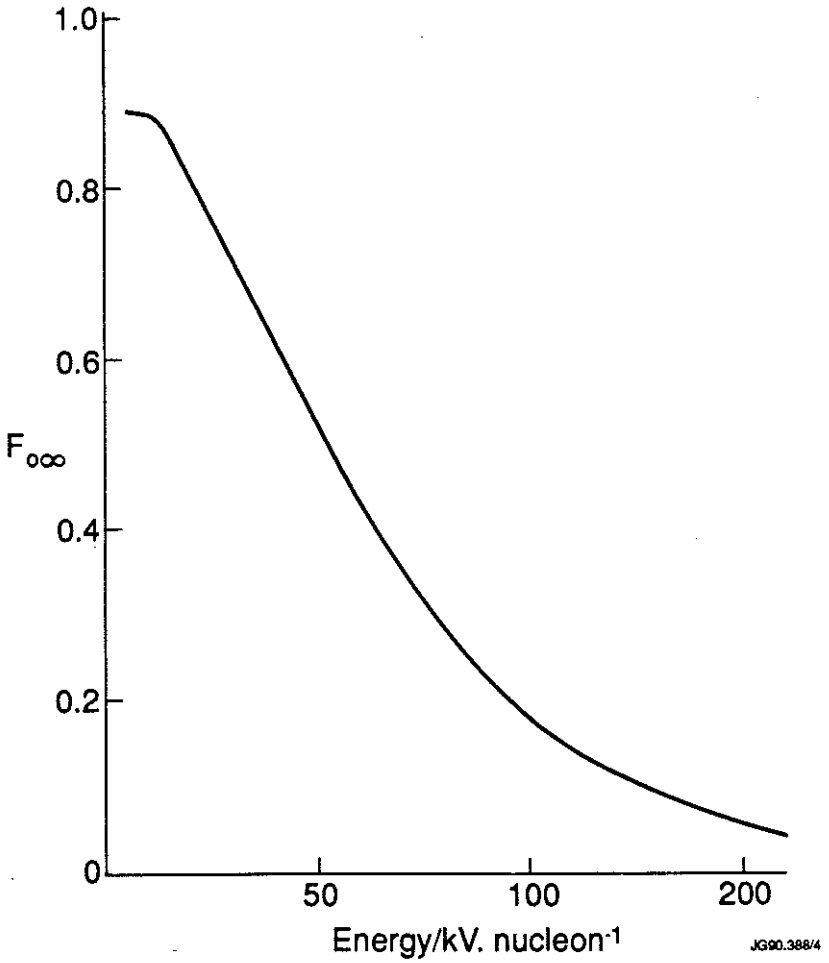

1. **Equilibrium Neutral Fraction ($F_{0\infty}$) versus Beam Energy for a Hydrogen Beam through Hydrogen Gas.**

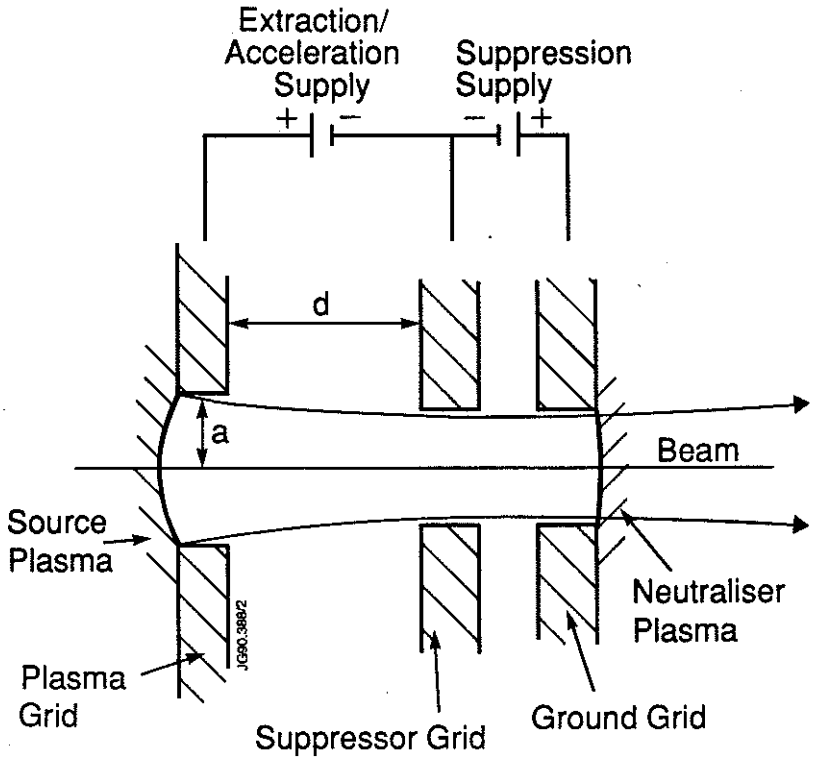

2. **Three grid Positive Ion Extraction System.**

The CLEO Source :

Anode diameter	120
Extraction electrodes diameter	80
Number of apertures	349
Extraction aperture diameter	3.7
Suppressor aperture diameter	2.8
Ground aperture diameter	2.8
Extraction to suppressor grid spacing	5
Supressor to ground grid spacing	1.5

(All dimensions in mm)

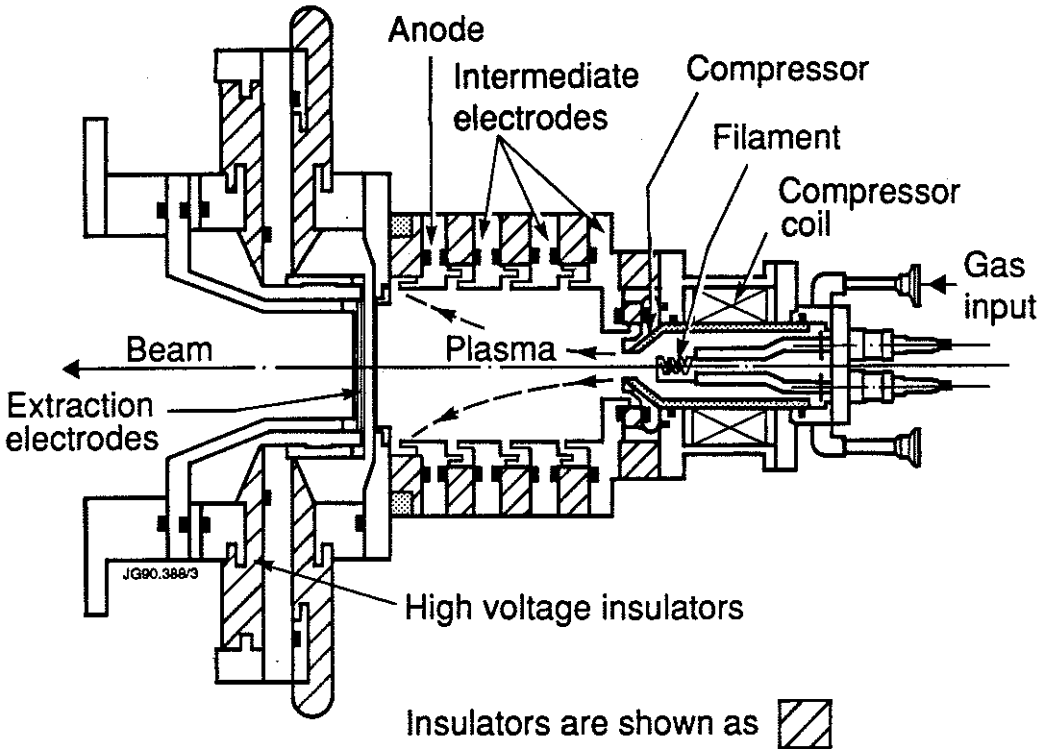

3. The CLEO Source.

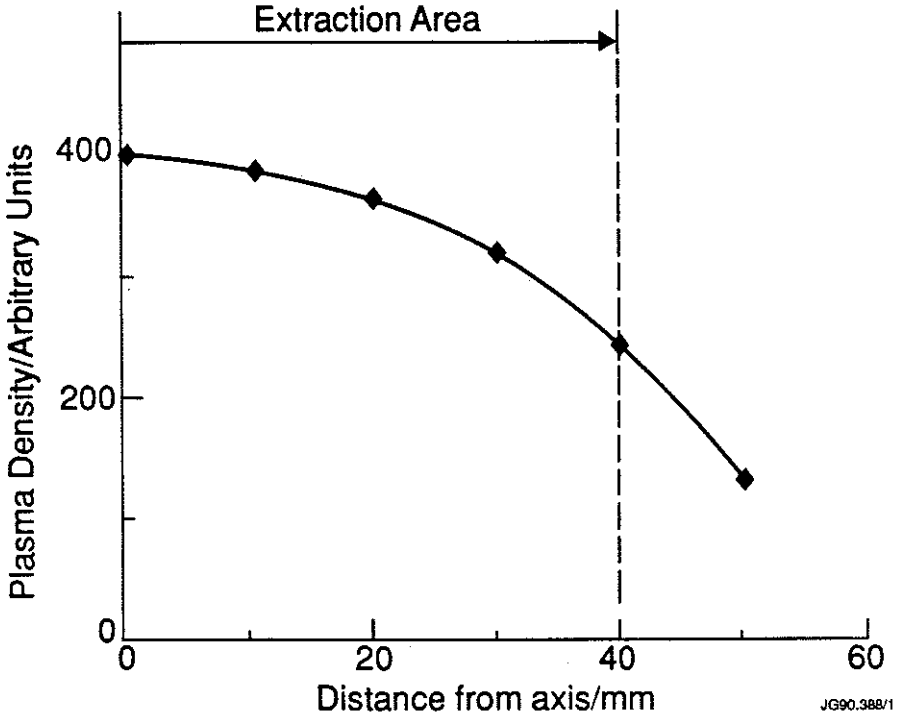

4. Plasma Density Distribution for the CLEO Source

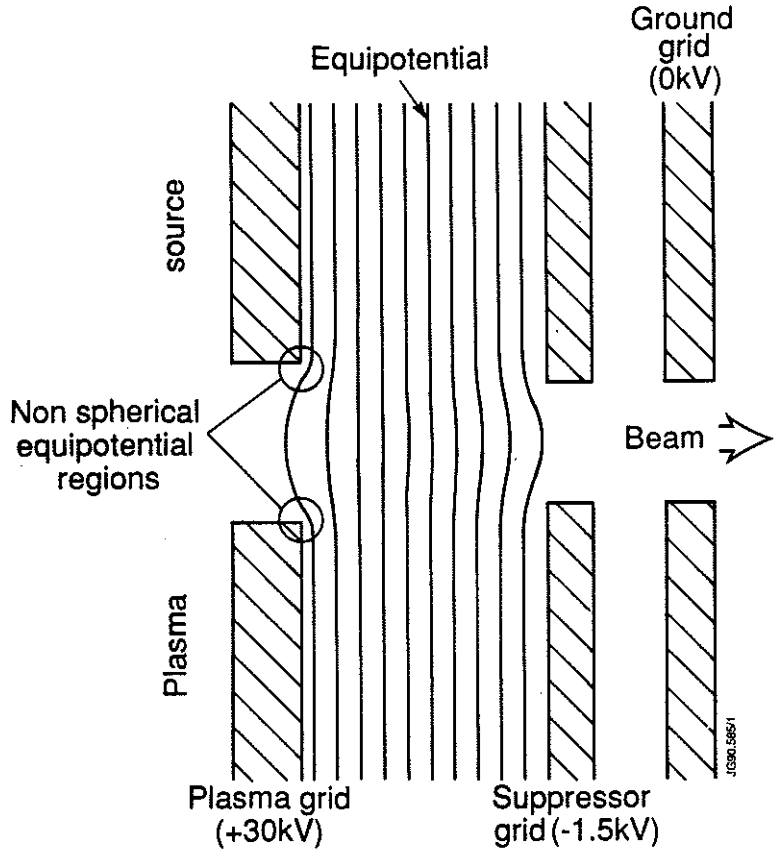

5a. Equipotentials Within a Three Grid, Cylindrical Aperture Positive Ion Extraction System.

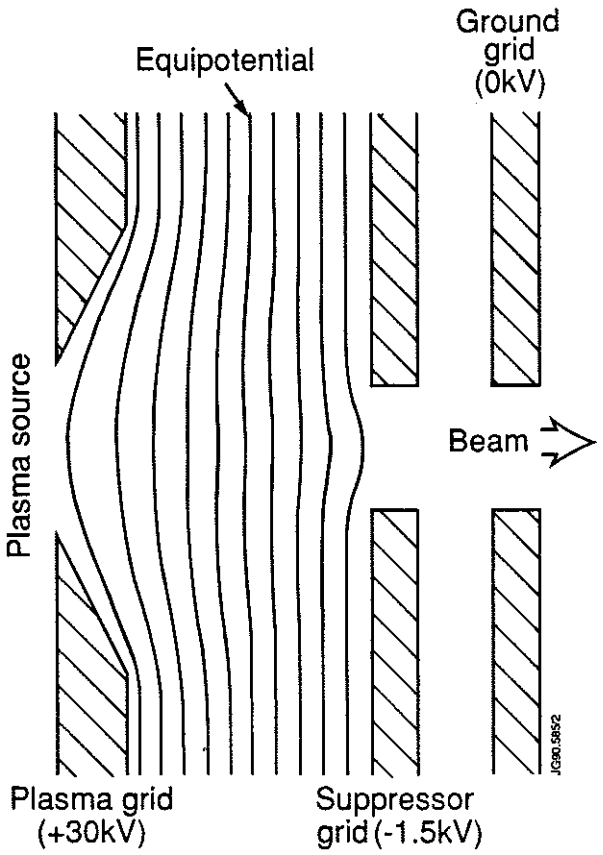

5b. shaped aperture.

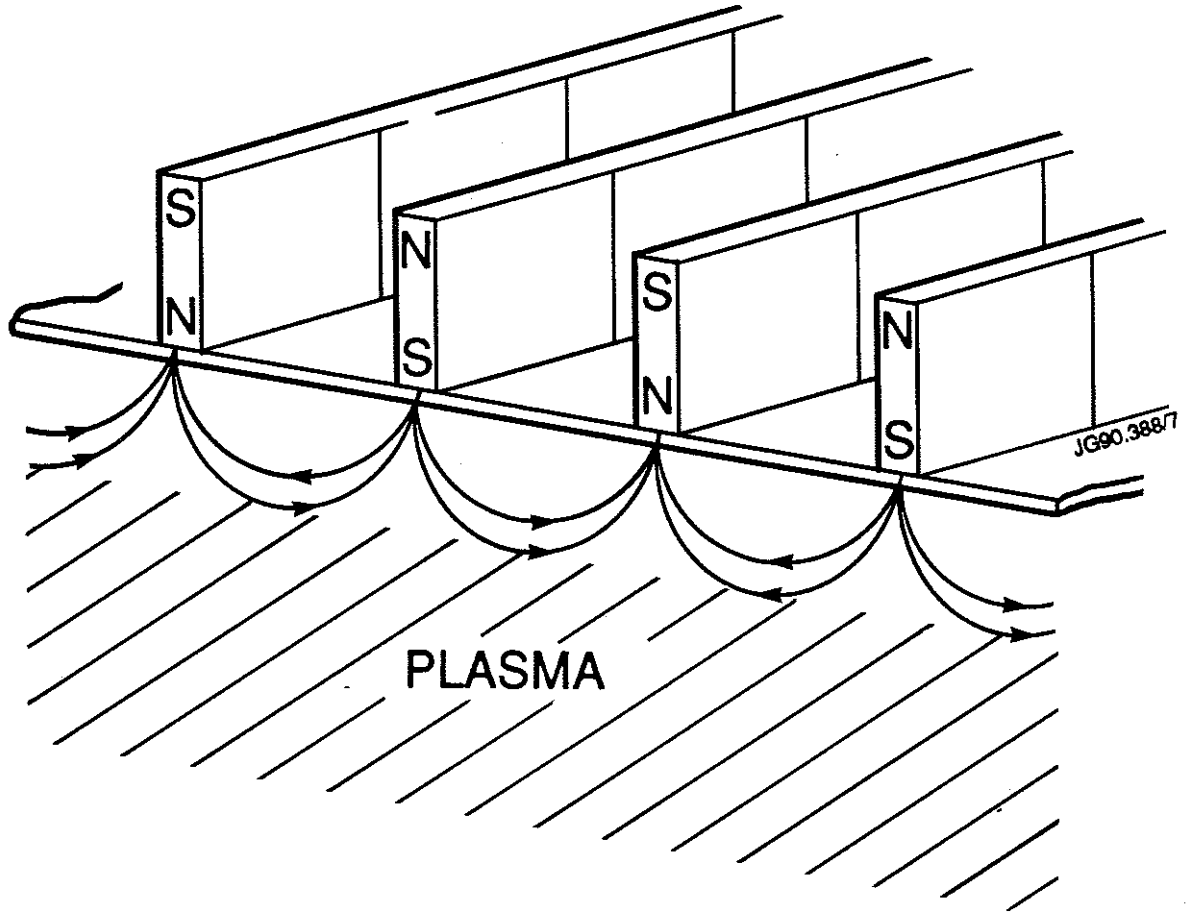

6. Multipole Permanent Magnet Line Cusp Confinement System.

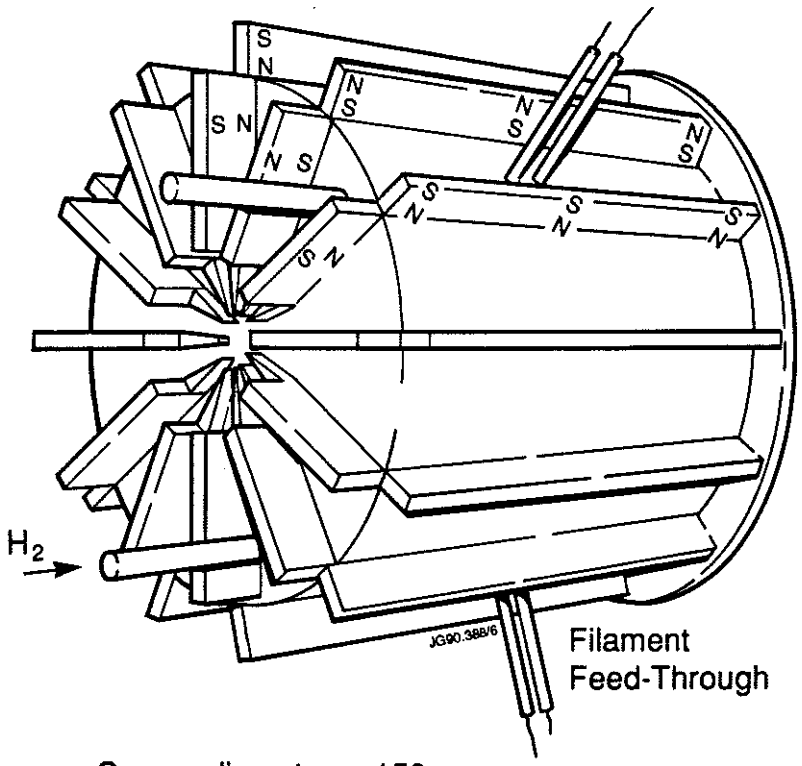

Source diameter =150mm
Source length =150mm

7a. Prototype Cylindrical "Bucket" Source.

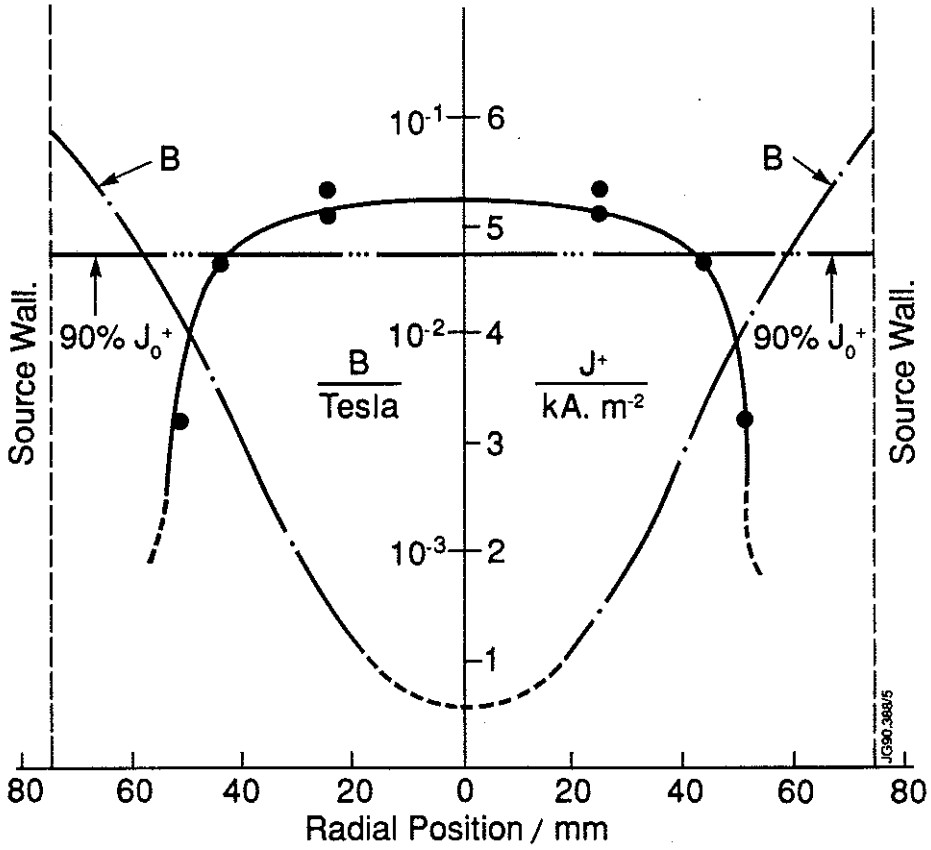

J+ =Ion current density to the extraction plane.
J0+ =J+ on axis.

7b. Plasma Density and Magnetic Field Distribution in the Prototype Bucket Source.

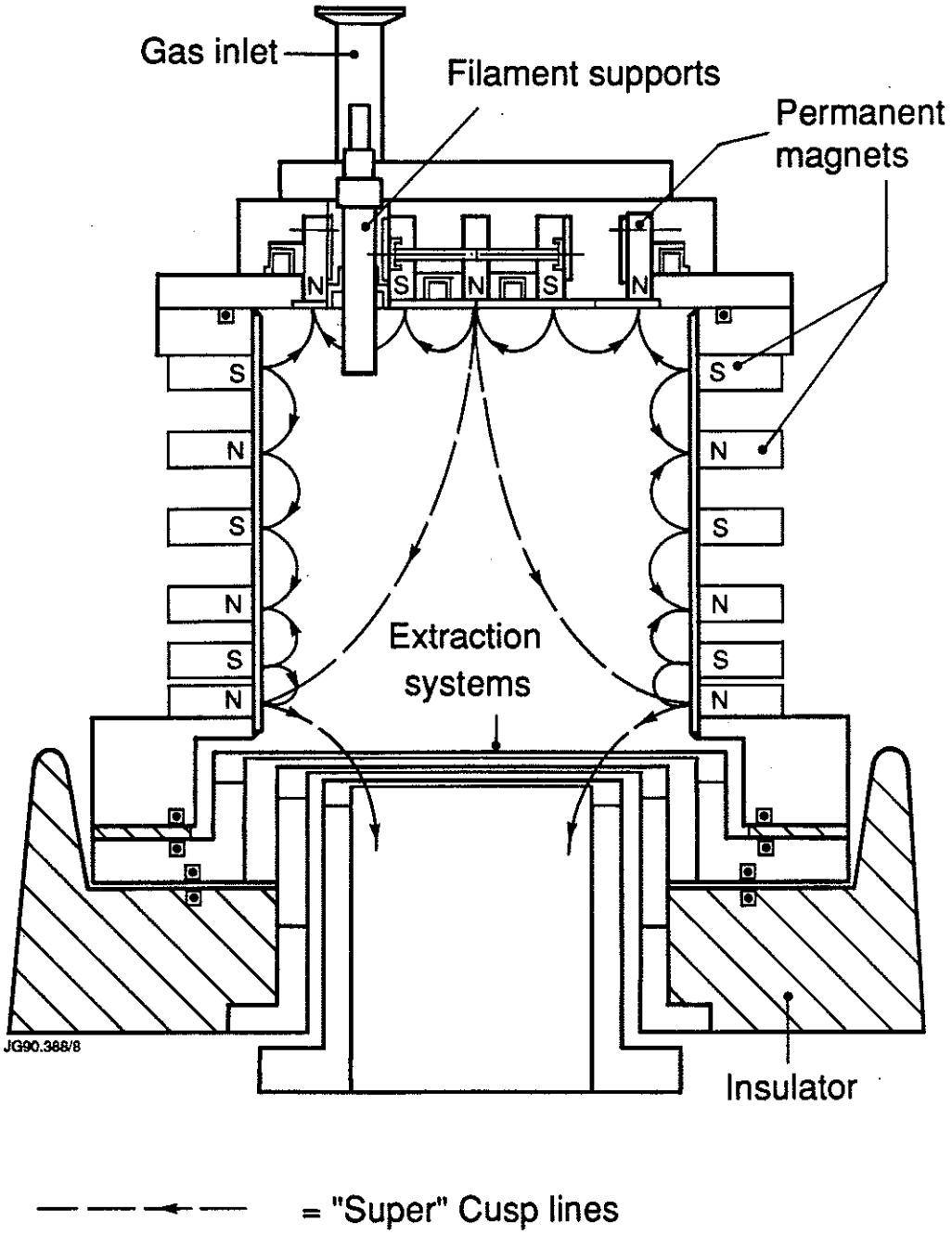

8a. Schematic Cross Section of the DITE Phase II Source.

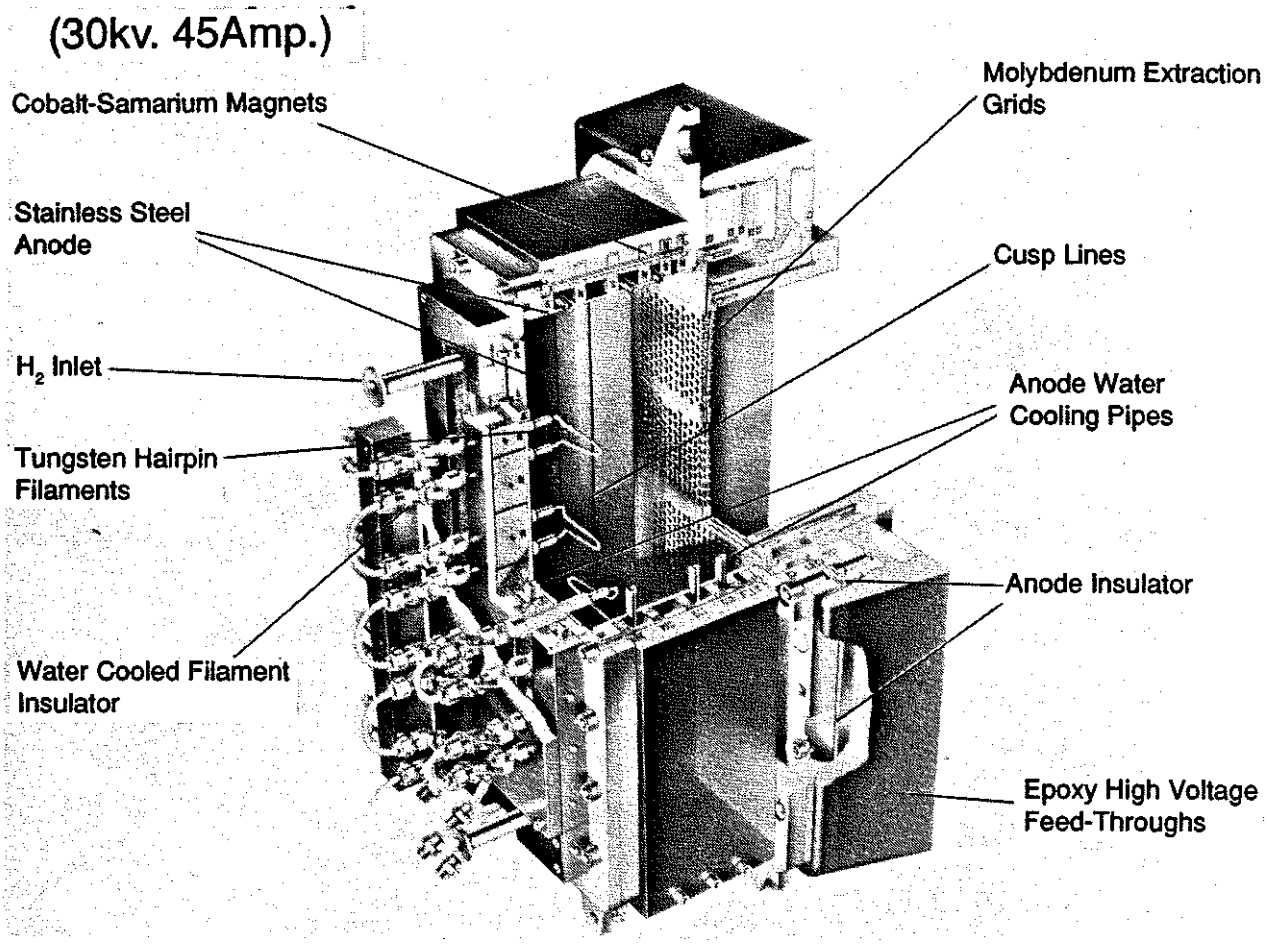

8b. DITE Phase II artists impression.

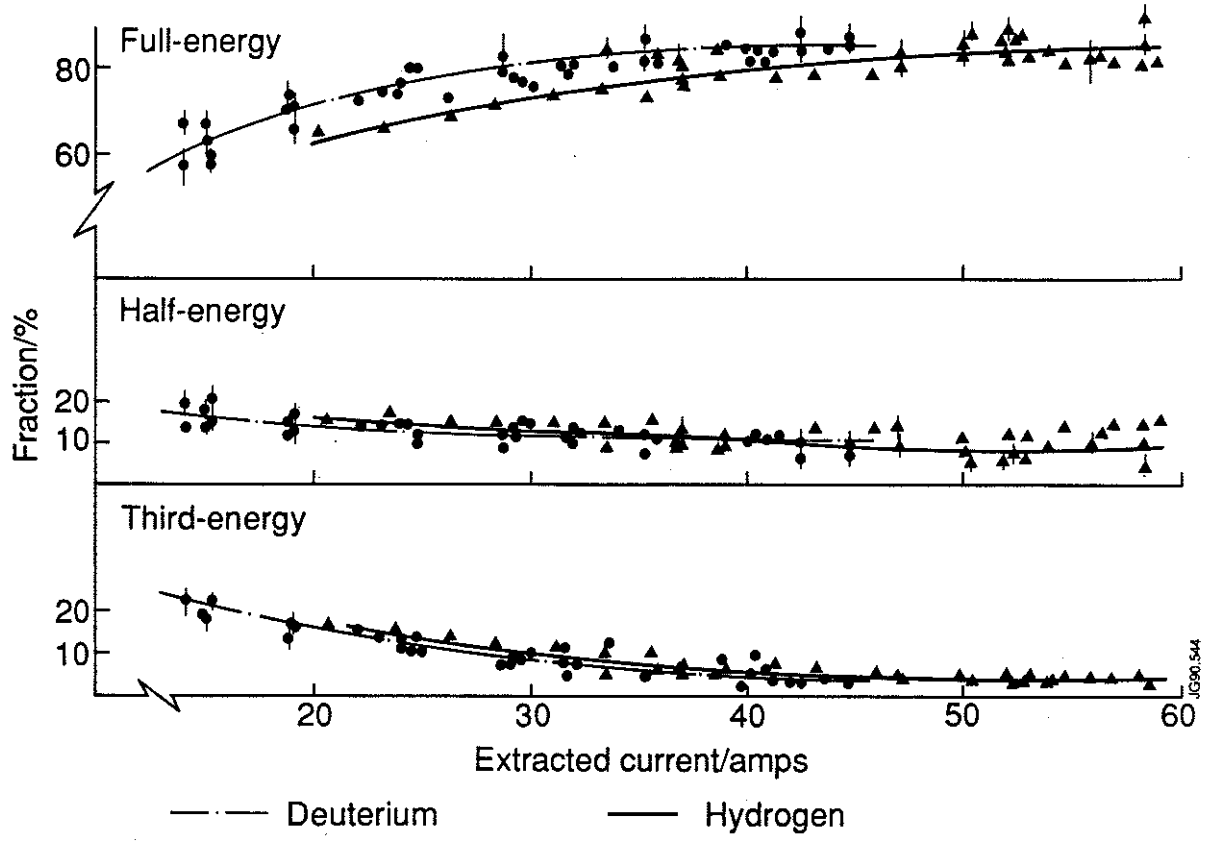

9. JET source species.

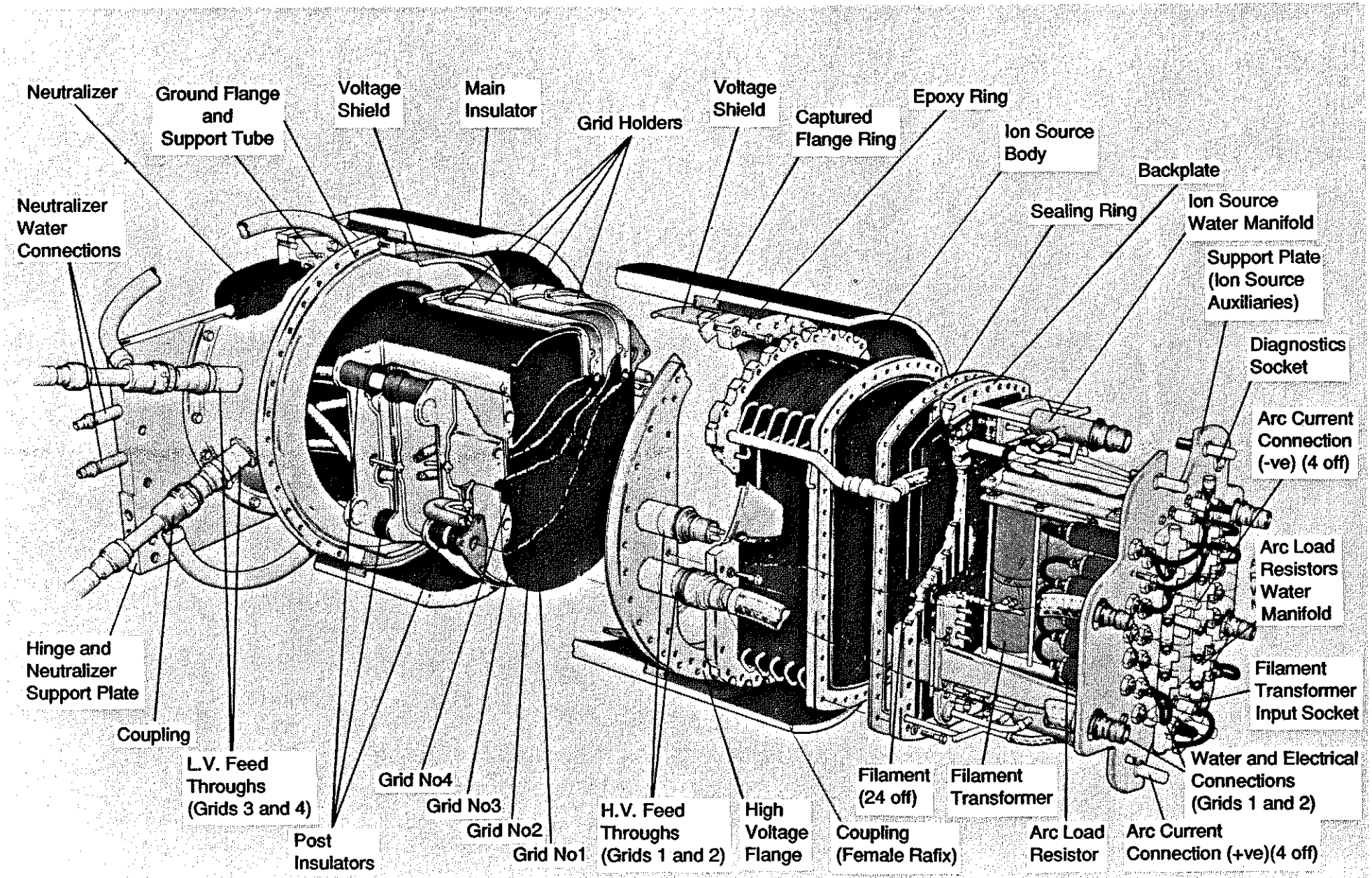

10. JET source schematic blow up.

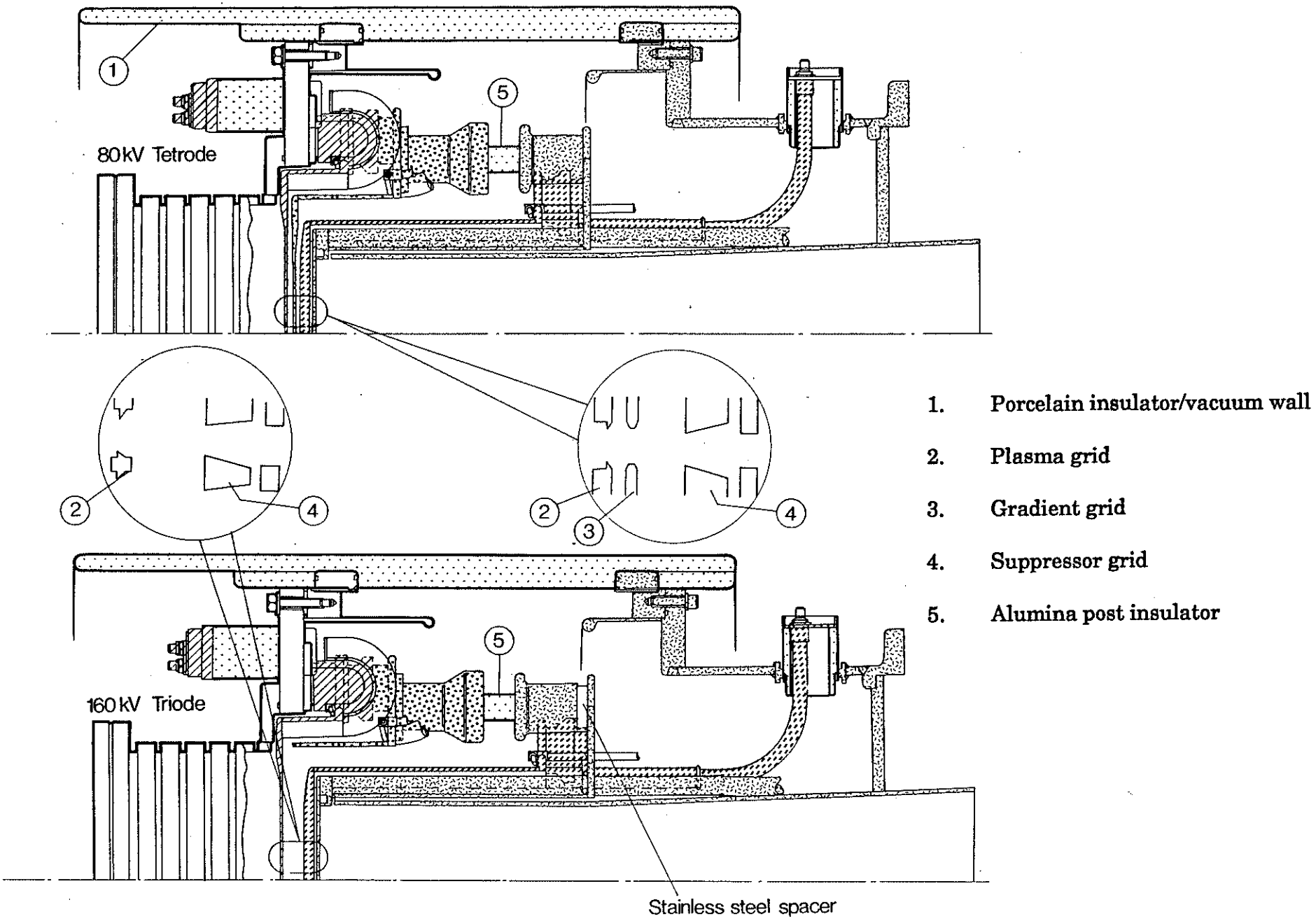

1. Porcelain insulator/vacuum wall
2. Plasma grid
3. Gradient grid
4. Suppressor grid
5. Alumina post insulator

11. JET triode and tetrode extraction systems

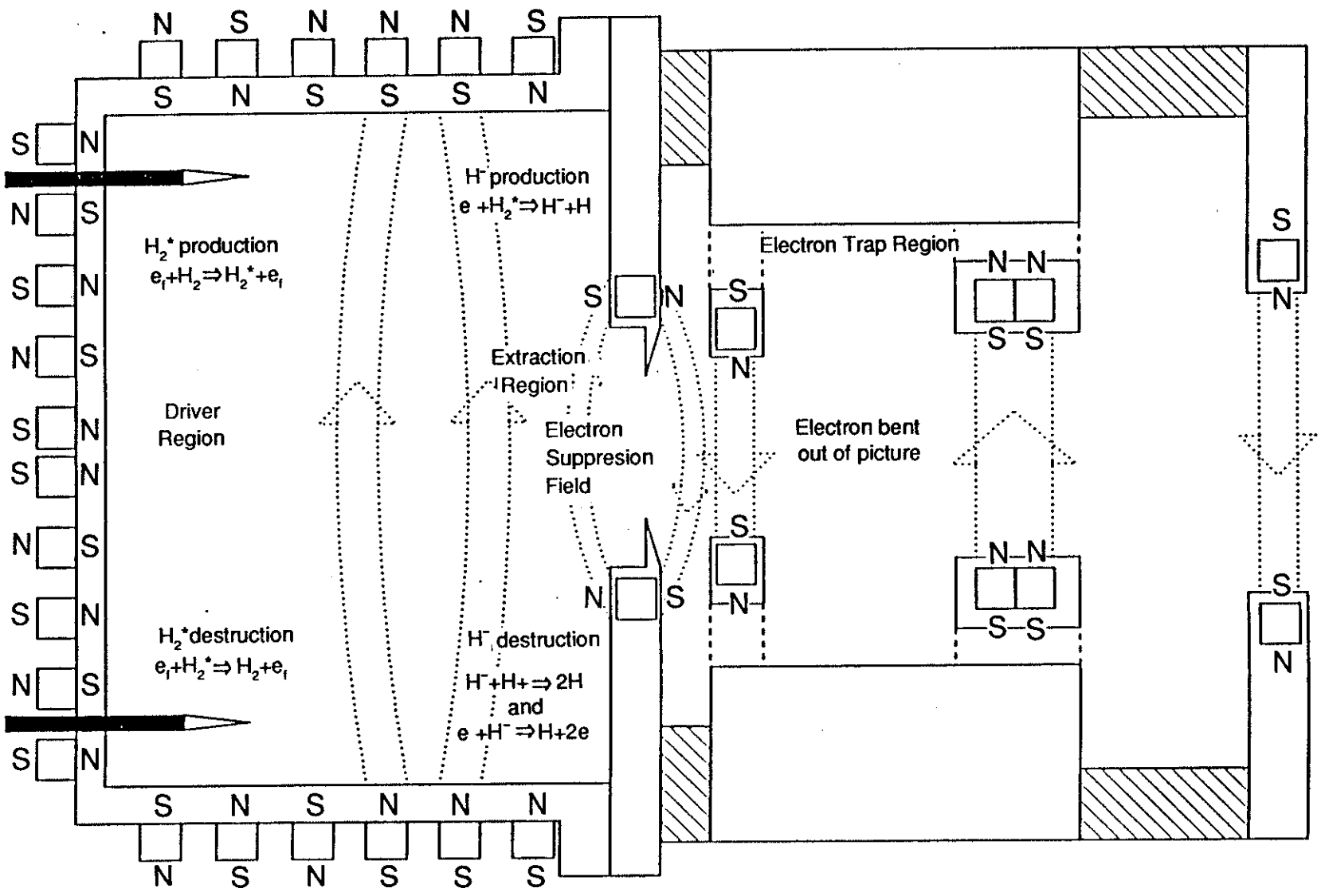

12. Schematic drawing of a conceptual H^-/D^- source.

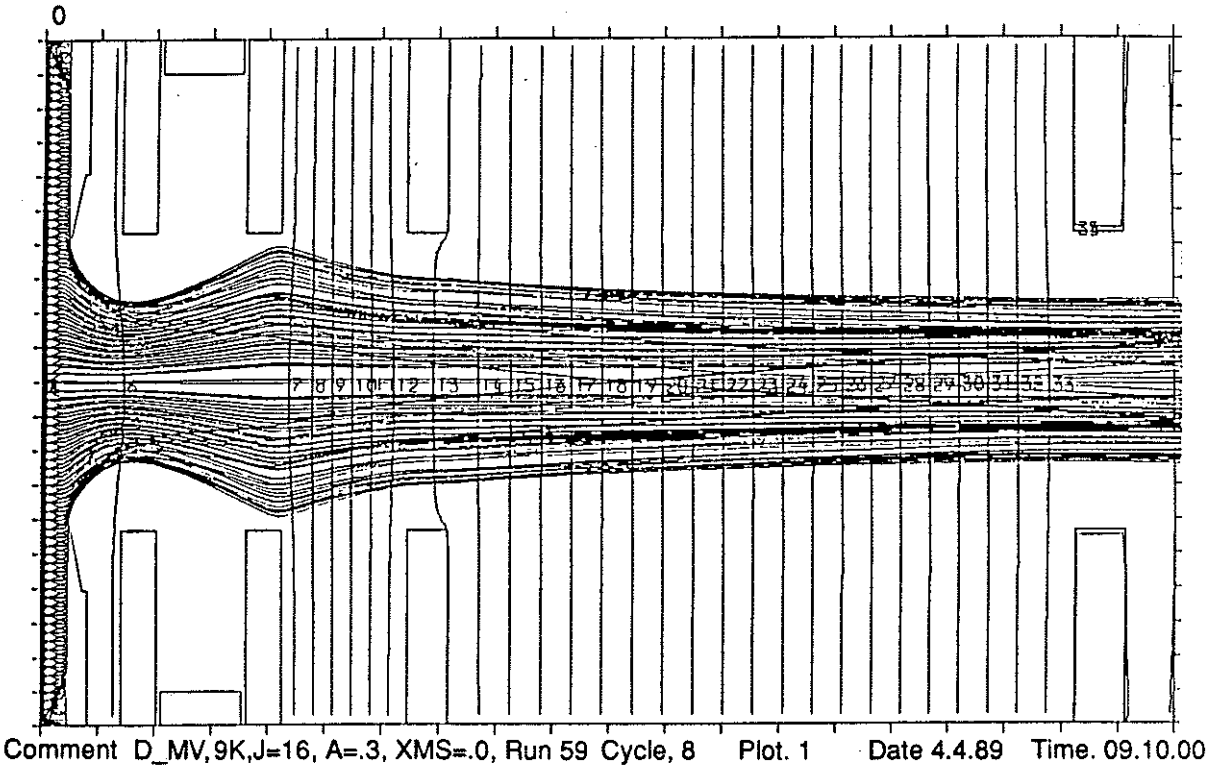

13. Ion Trajectories for the 200 kV D^- accelerator. Beam focusing is controlled by the potential across first two gaps only.

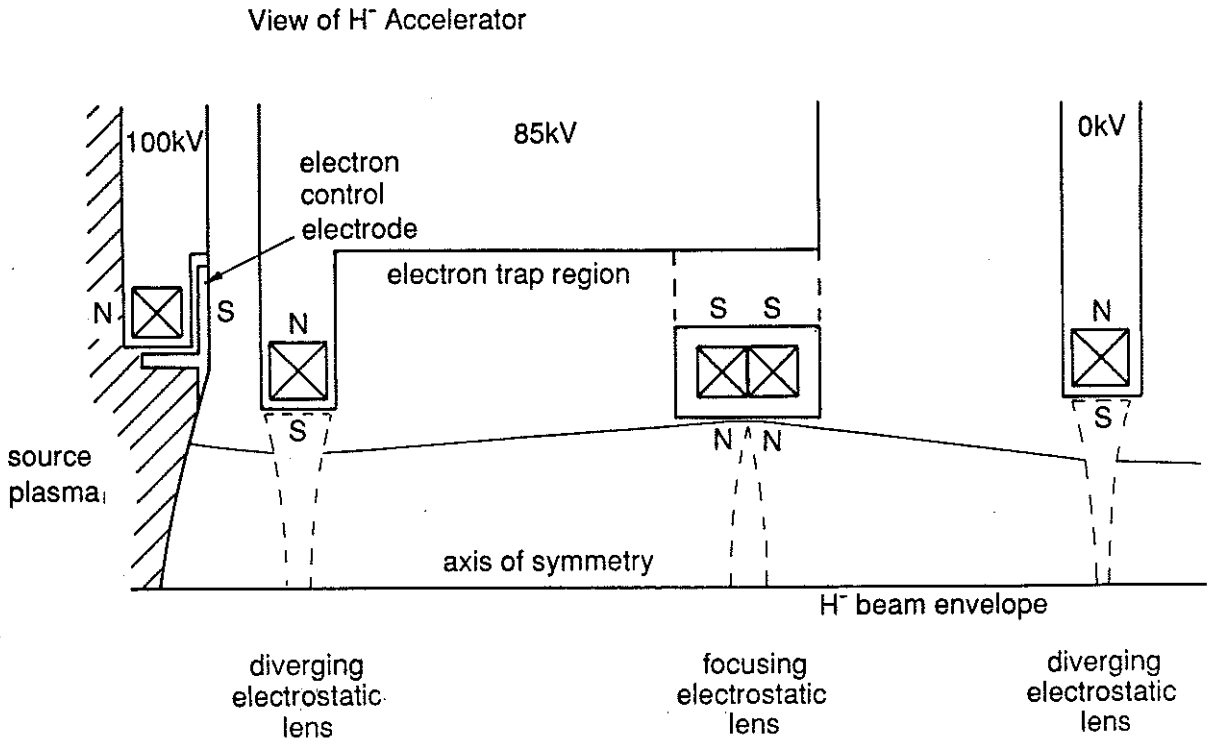

14. Illustration of focusing and electron deflection fields within the accelerator structure.

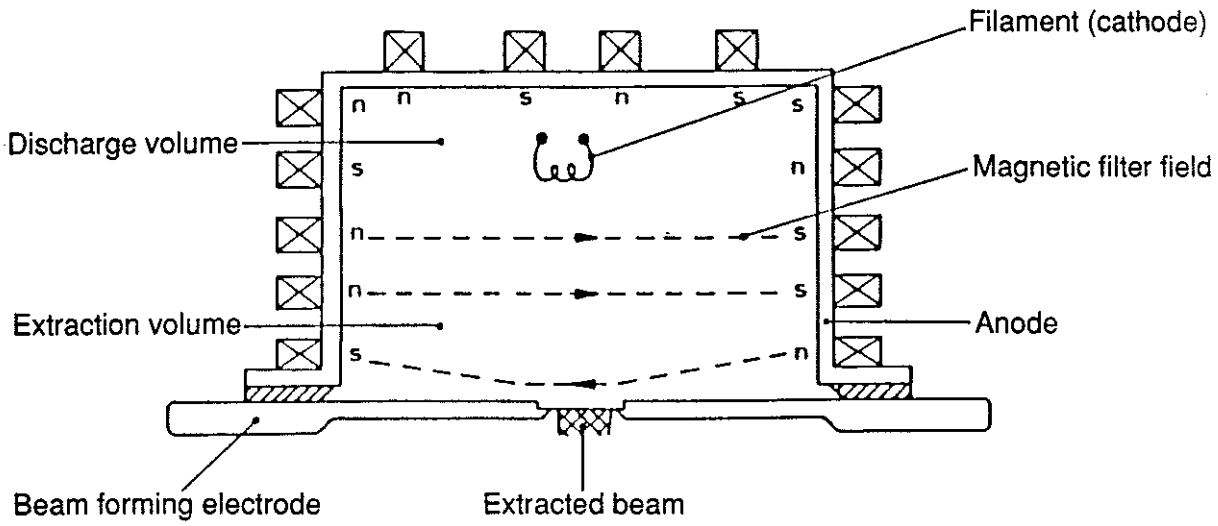

15. Cross Section Diagram of the Prototype Negative Ion Source (1982 version).

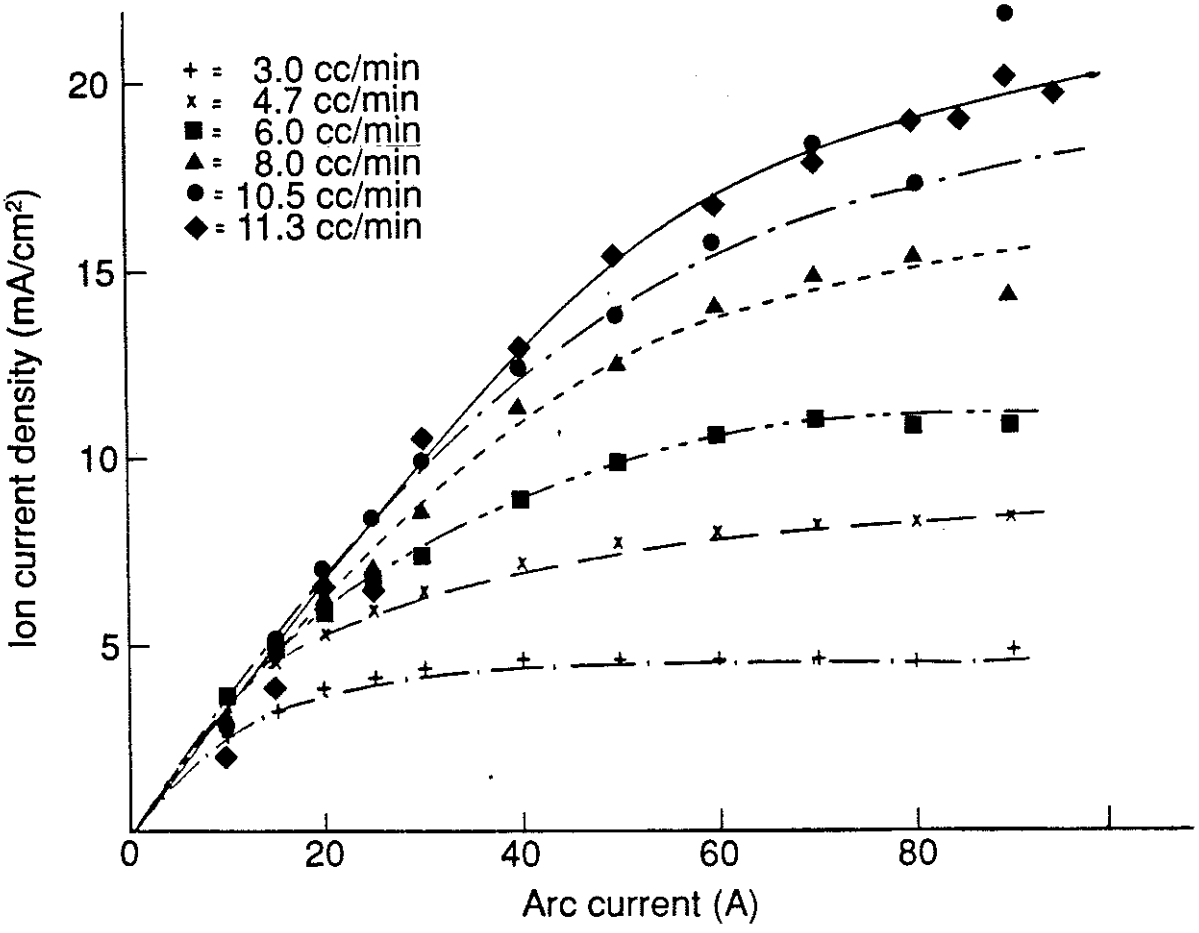

16. Variation of Negative Ion Current Density with Pressure and Arc Current in the Prototype Source.

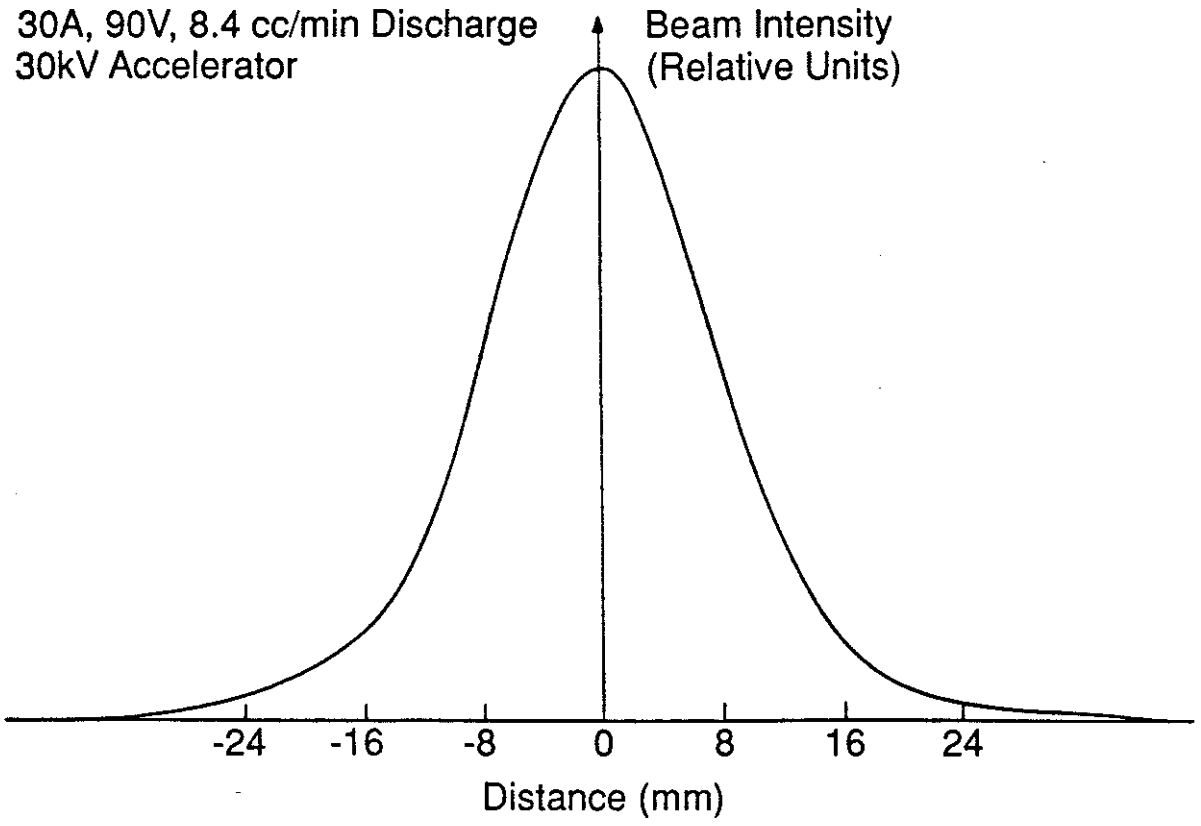

17. Beam Profile for Optimum Collimation of a Negative Ion Beam.

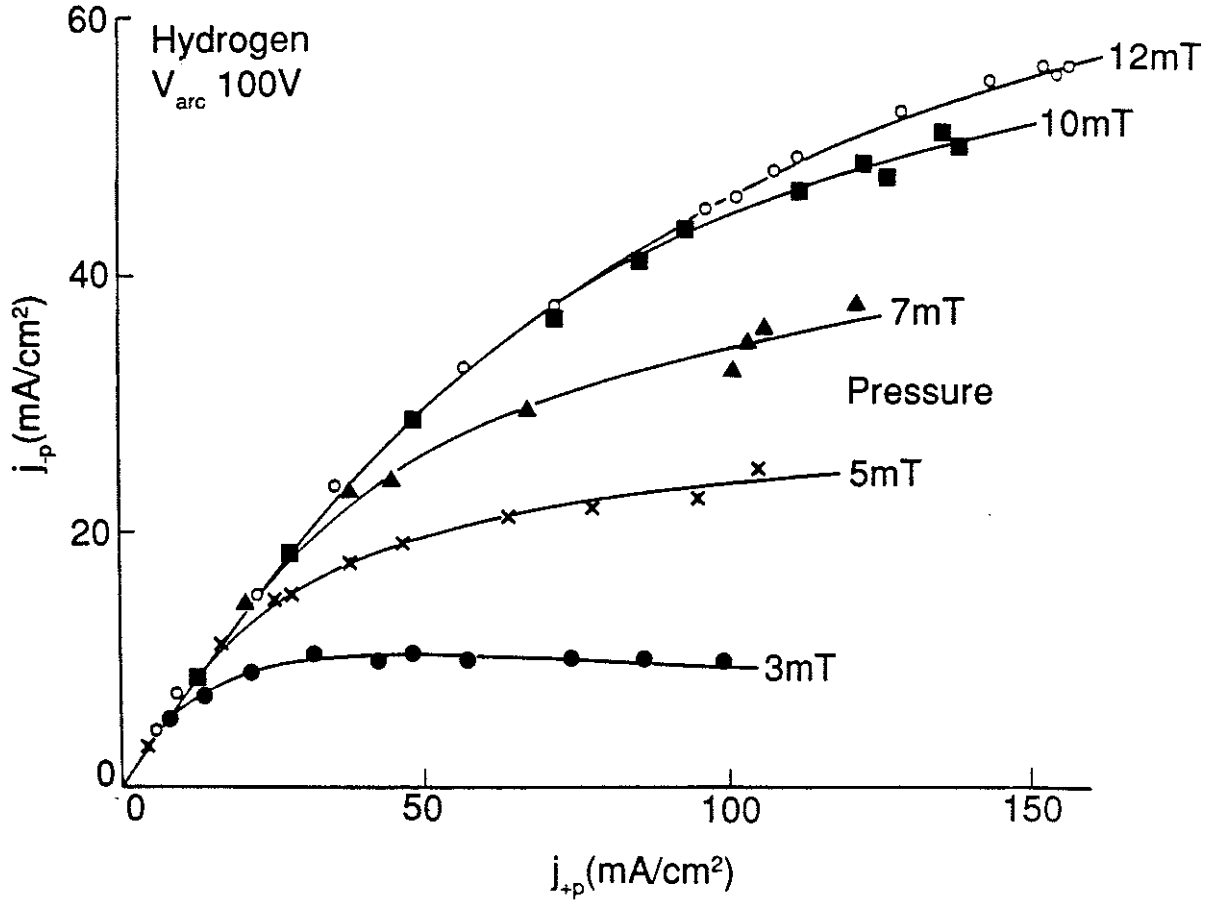

18. Variation of H^- Current Density with Arc Power and Pressure in the 55 x 31 x 21 cm^3 source.

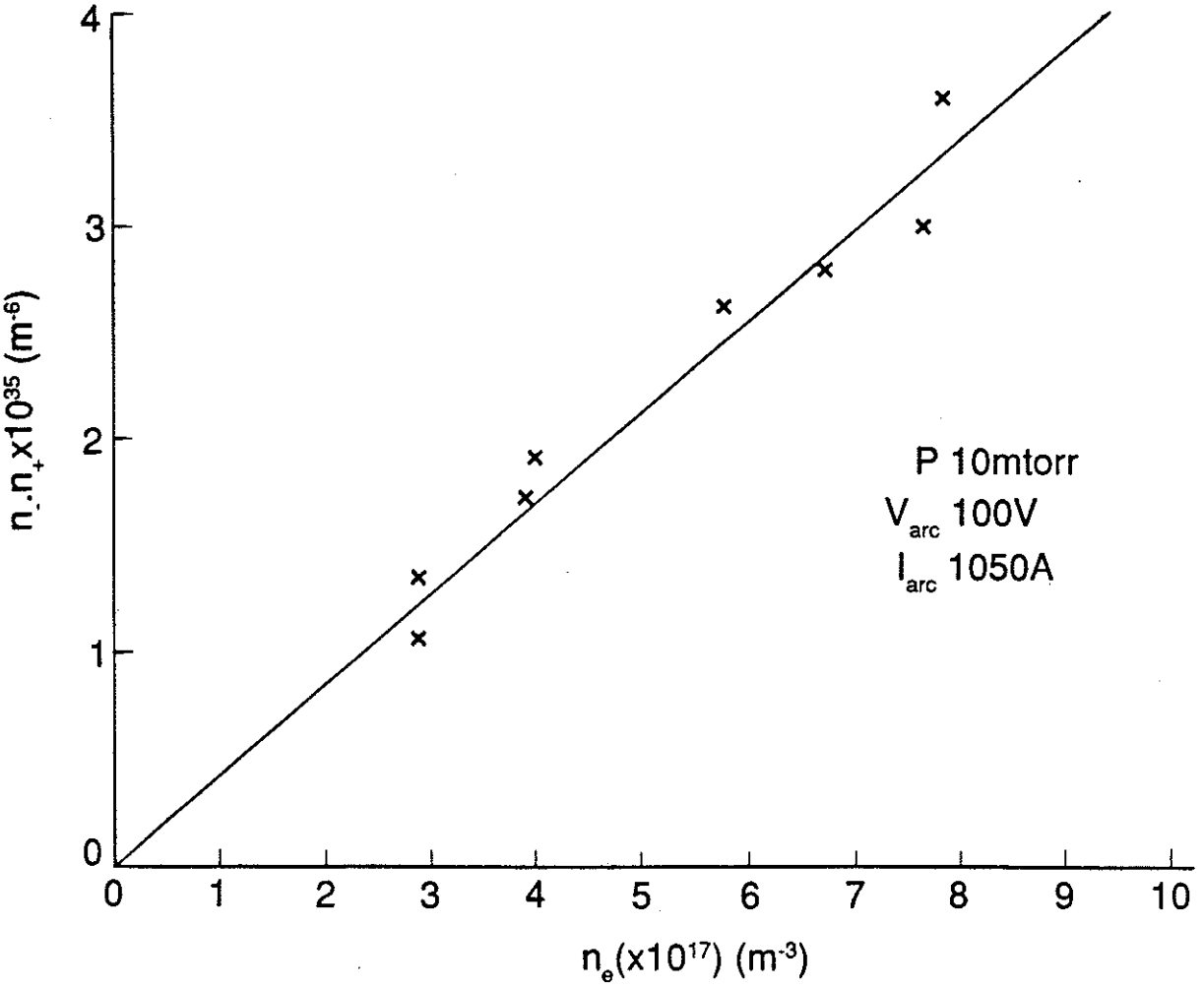

19. Plot of n_+ n_- Versus n_e for the 55 x 31 x 21 cm^3 Source Confirming Ion-Ion Recombination Loss as the Dominant Channel at High Power.

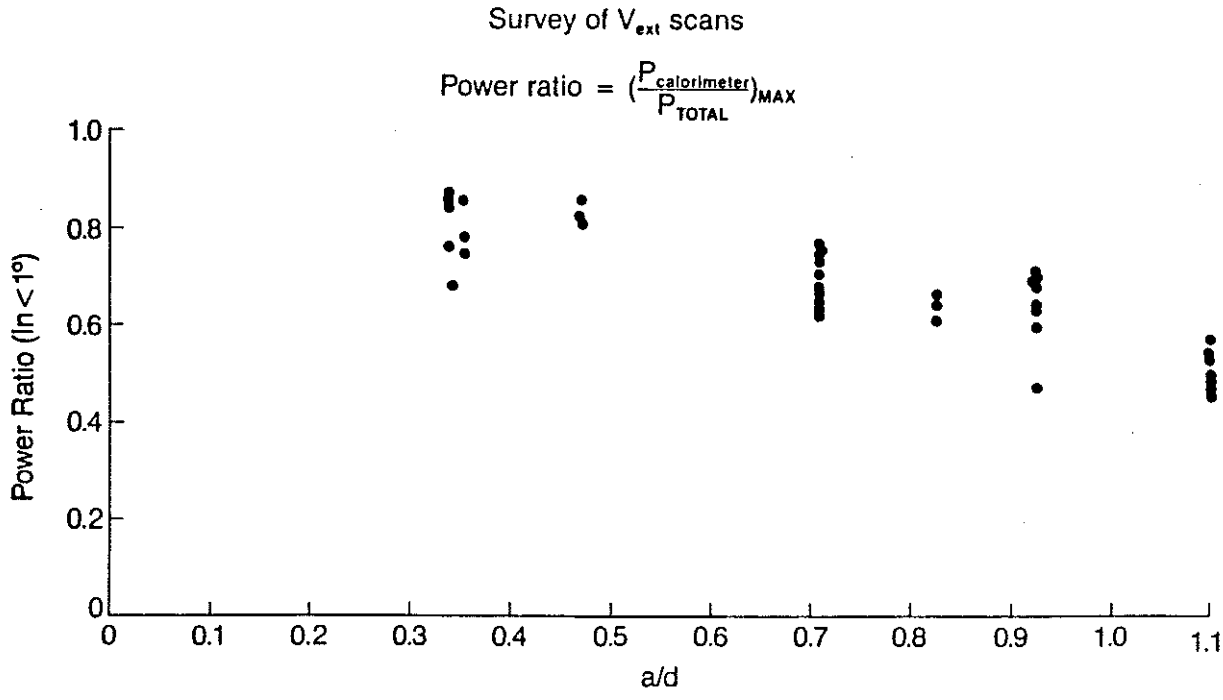

20. Measurement of the Beam Halo Power Versus Aspect Ratio (a/d) of the First Gap of the Accelerator.

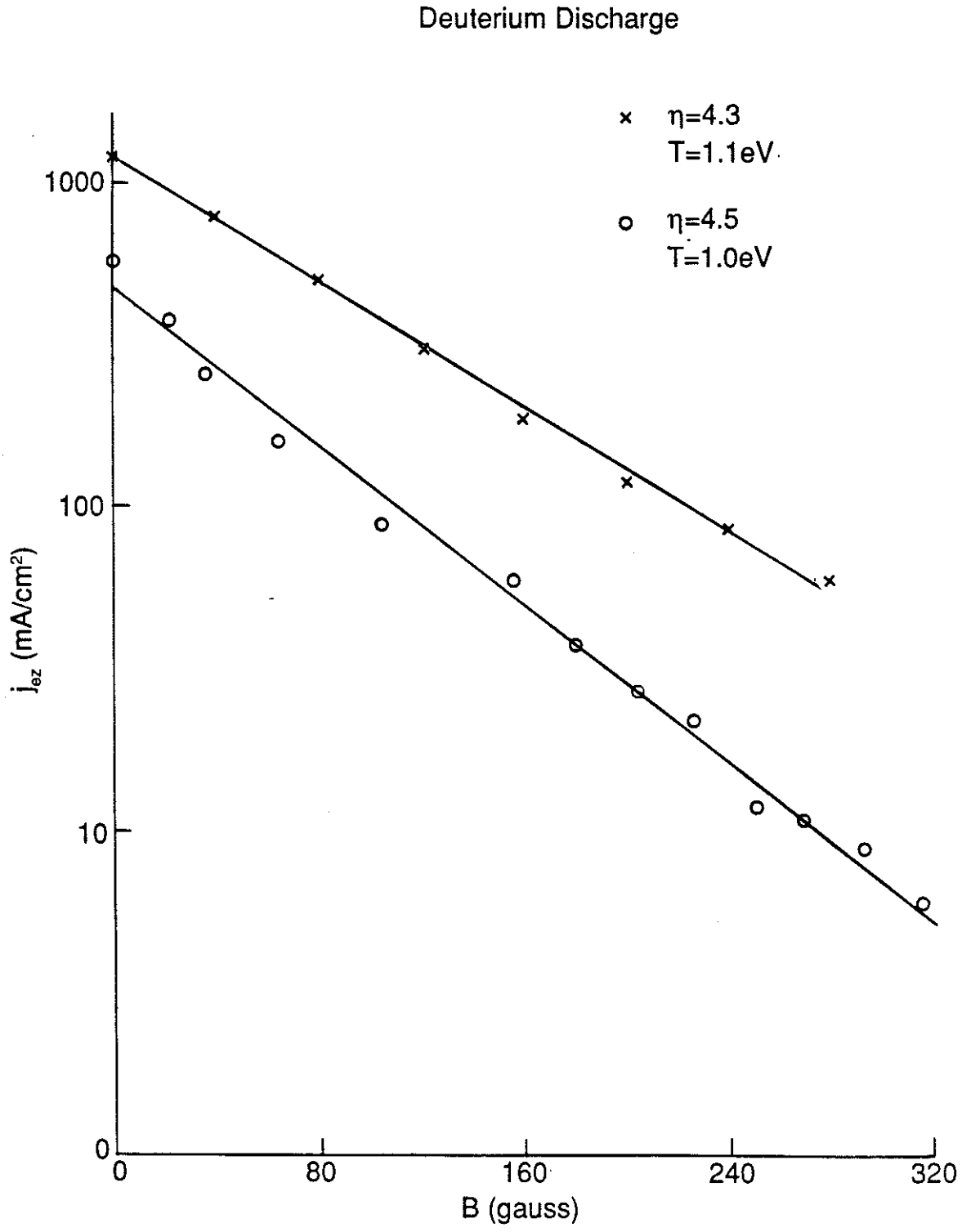

21. Extracted Electron Current Versus Magnetic Suppression Field for D^- Beam Operation.

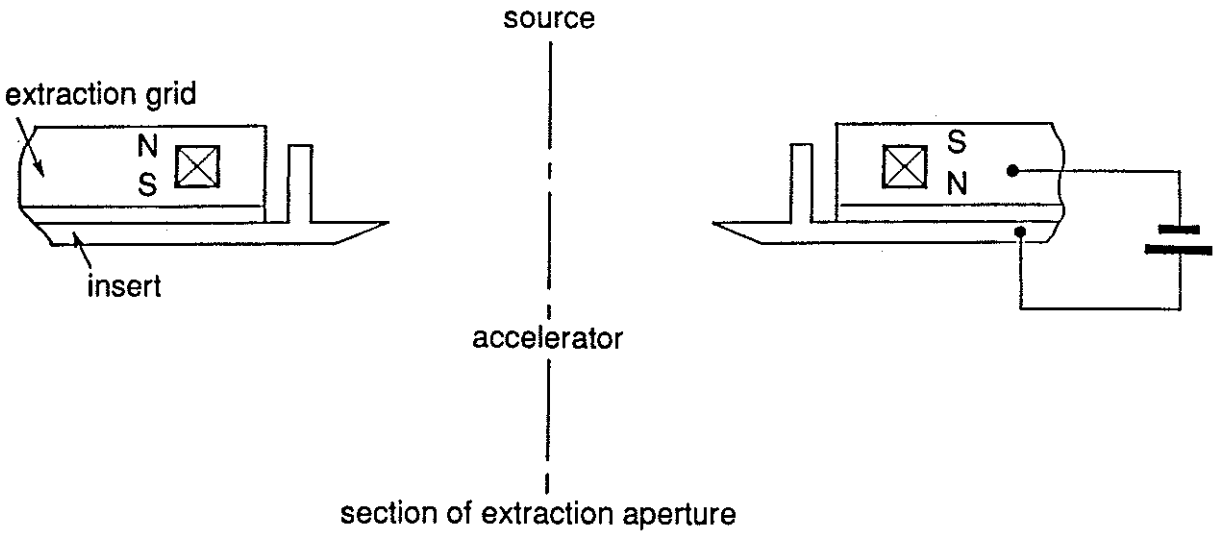

22. **Permanent Magnet Suppression System for Electrons. The Electrons are Collected on the Sidewalls Adjacent to the Aperture.**

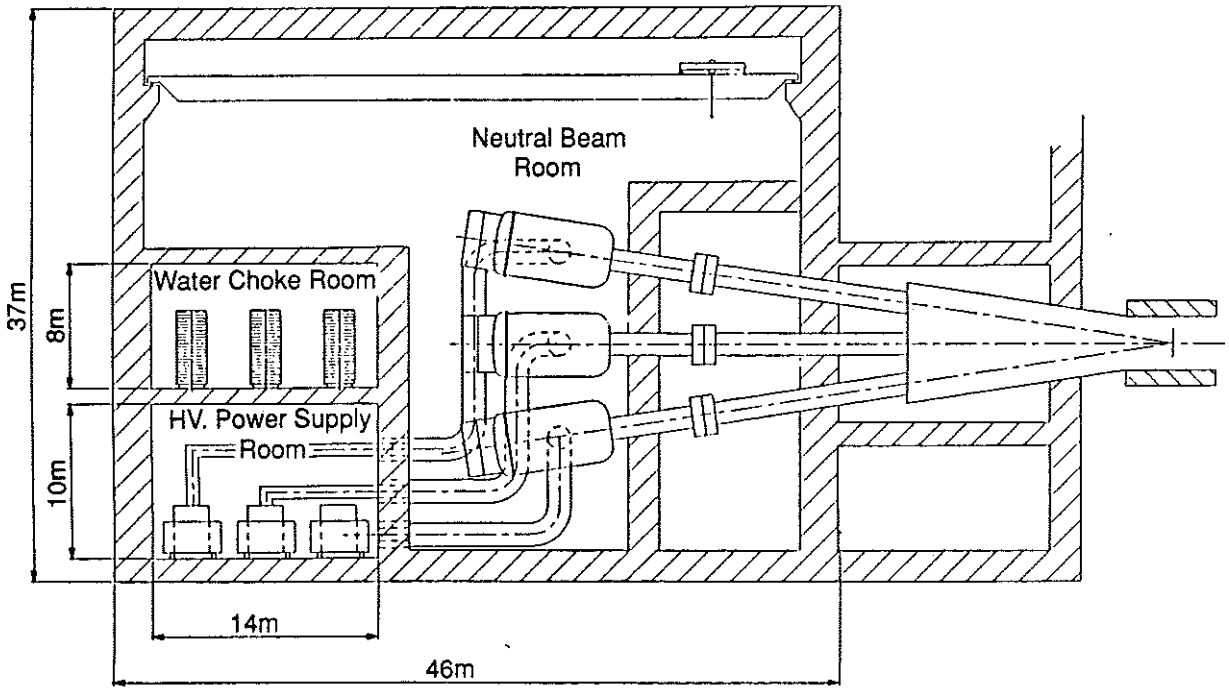

23. **Elevation View of the ITER/NET Injector System for 1.3 MeV D° Beams. Each Module Delivers 8.3 MW of Power and a Peak Power of up to 10 MW.**

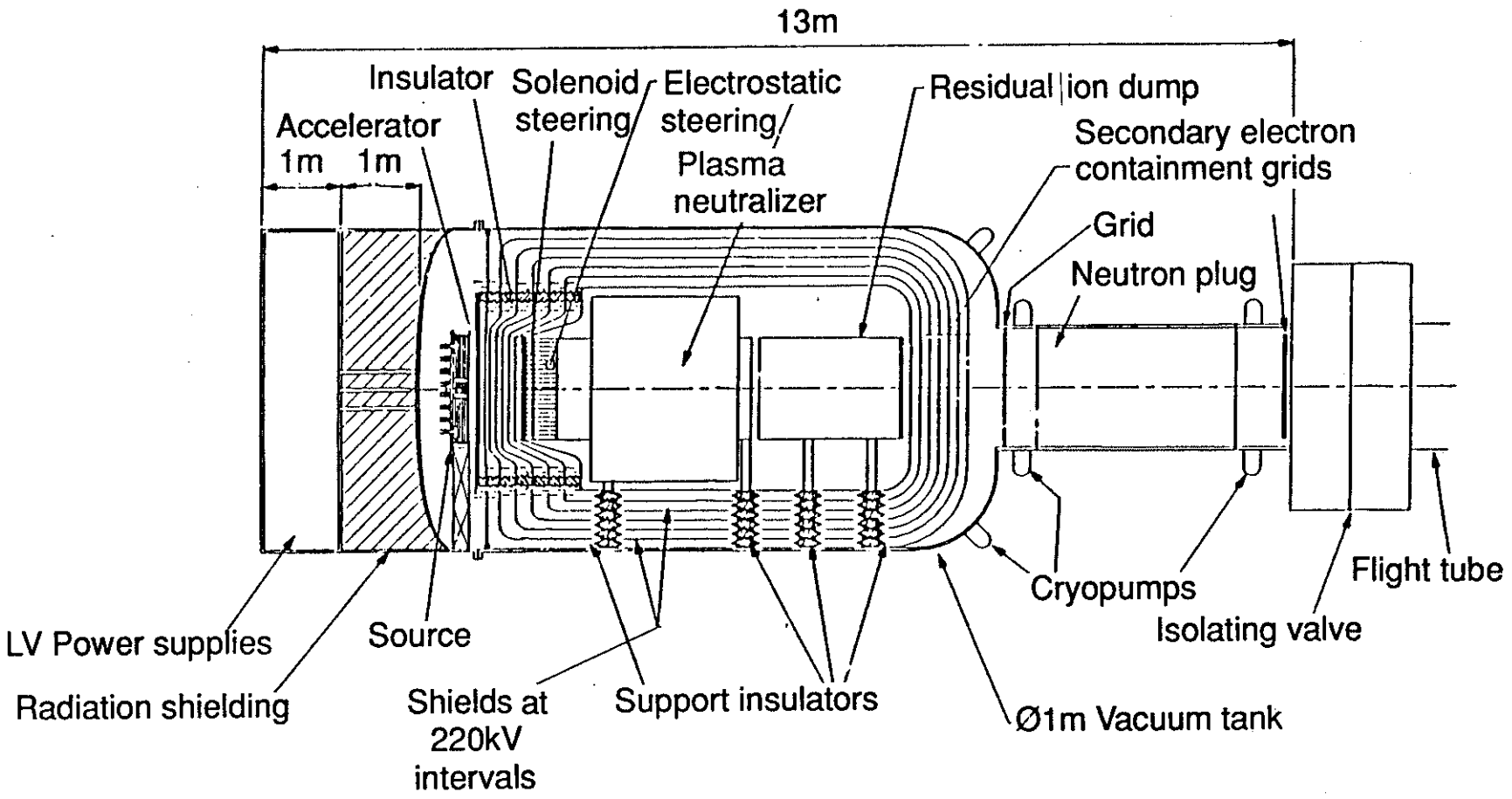

24. Interior View of One Module. There are Two Sources, Accelerators and Neutraliser Assemblies Side by Side in the Module.

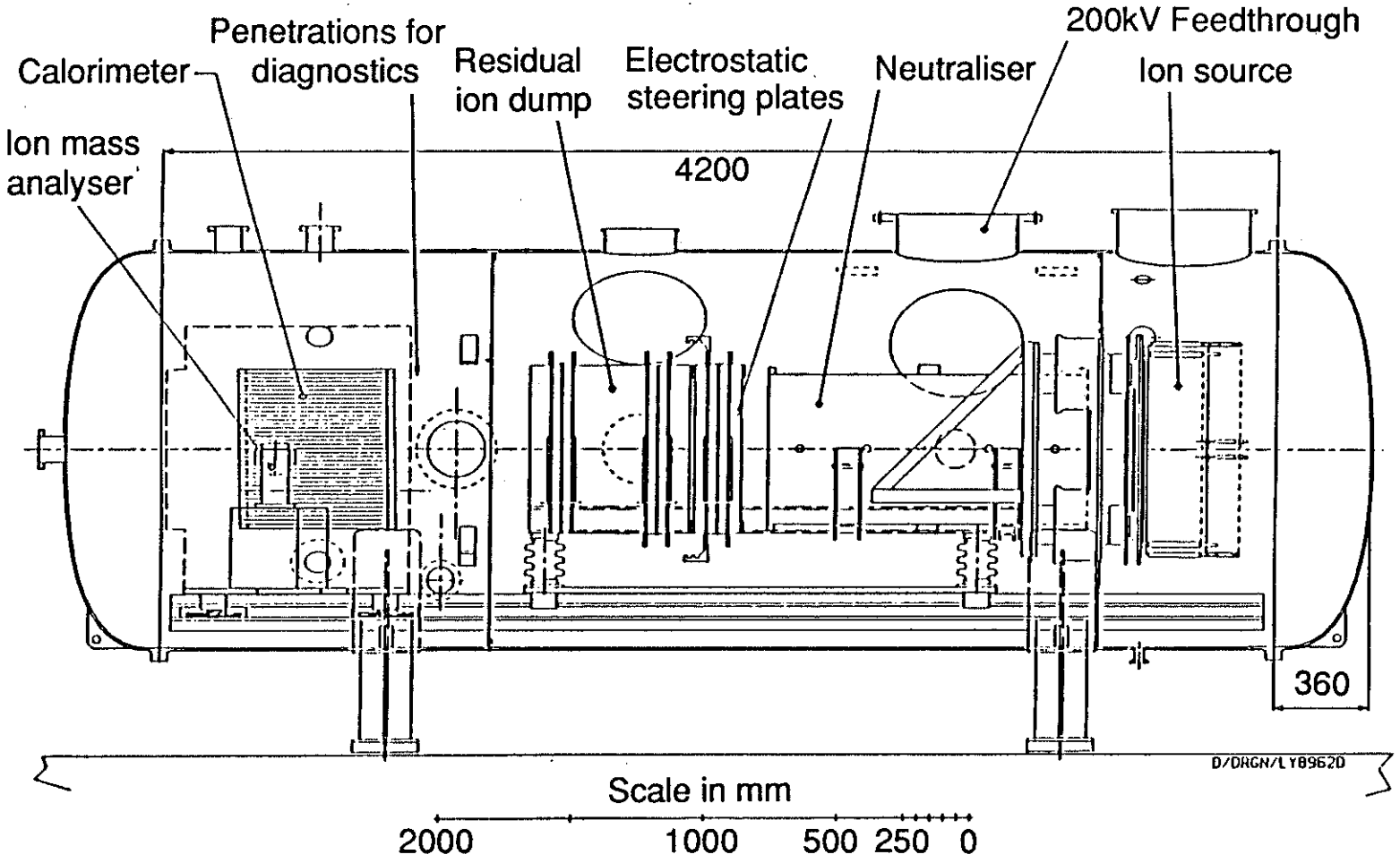

25. **Interior View of the Prototype Unit Which Operates at 200 keV, 4 A of D⁻.**

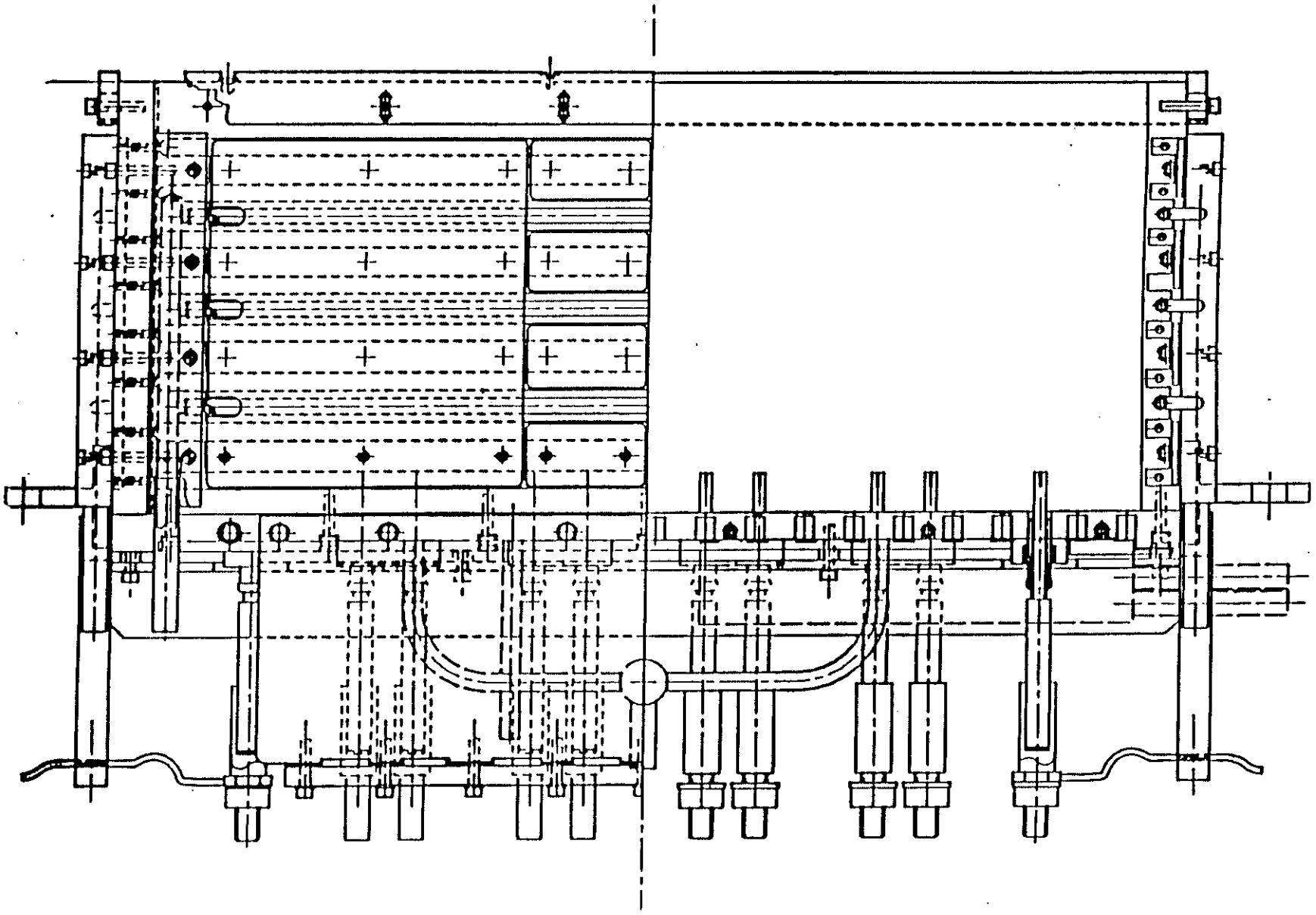

26. View of the Plasma Source of the Prototye D^- Injector. This 2/3 of the Full Scale Unit.

APPENDIX 1.

THE JET TEAM

JET Joint Undertaking, Abingdon, Oxon, OX14 3EA, U.K.

J.M.Adams[1], F.Alladio[4], H.Altmann, R.J.Anderson, G.Appruzzese, W.Bailey, B.Balet, D.V.Bartlett, L.R.Baylor[24], K.Behringer, A.C.Bell, P.Bertoldi, E.Bertolini, V.Bhatnagar, R.J.Bickerton, A.Boileau[3], T.Bonicelli, S.J.Booth, G.Bosia, M.Botman, D.Boyd[31], H.Brelen, H.Brinkschulte, M.Brusati, T.Budd, M.Bures, T.Businaro[4], H.Buttgereit, D.Cacaut, C.Caldwell-Nichols, D.J.Campbell, P.Card, J.Carwardine, G.Celentano, P.Chabert[27], C.D.Challis, A.Cheetham, J.Christiansen, C.Christodoulopoulos, P.Chuilon, R.Claesen, S.Clement[30], J.P.Coad, P.Colestock[6], S.Conroy[13], M.Cooke, S.Cooper, J.G.Cordey, W.Core, S.Corti, A.E.Costley, G.Cottrell, M.Cox[7], P.Cripwell[13], F.Crisanti[4], D.Cross, H.de Blank[16], J.de Haas[16], L.de Kock, E.Deksnis, G.B.Denne, G.Deschamps, G.Devillars, K.J.Dietz, J.Dobbing, S.E.Dorling, P.G.Doyle, D.F.Düchs, H.Duquenoy, A.Edwards, J.Ehrenberg[14], T.Elevant[12], W.Engelhardt, S.K.Erents[7], L.G.Eriksonn[5], M.Evrard[2], H.Falter, D.Flory, M.Forrest[7], C.Froger, K.Fullard, M.Gadeberg[11], A.Galetsas, R.Galvao[8], A.Gibson, R.D.Gill, A.Gondhalekar, C.Gordon, G.Gorini, C.Gormezano, N.A.Gottardi, C.Gowers, B.J.Green, F.S.Griph, M.Gryzinski[26], R.Haange, G.Hammett[6], W.Han[9], C.J.Hancock, P.J.Harbour, N.C.Hawkes[7], P.Haynes[7], T.Hellsten, J.L.Hemmerich, R.Hemsworth, R.F.Herzog, K.Hirsch[14], J.Hoekzema, W.A.Houlberg[24], J.How, M.Huart, A.Hubbard, T.P.Hughes[32], M.Hugon, M.Huguet, J.Jacquinot, O.N.Jarvis, T.C.Jernigan[24], E.Joffrin, E.M.Jones, L.P.D.F.Jones, T.T.C.Jones, J.Källne, A.Kaye, B.E.Keen, M.Keilhacker, G.J.Kelly, A.Khare[15], S.Knowlton, A.Konstantellos, M.Kovanen[21], P.Kupschus, P.Lallia, J.R.Last, L.Lauro-Taroni, M.Laux[33], K.Lawson[7], E.Lazzaro, M.Lennholm, X.Litaudon, P.Lomas, M.Lorentz-Gottardi[2], C.Lowry, G.Magyar, D.Maisonnier, M.Malacarne, V.Marchese, P.Massmann, L.McCarthy[28], G.McCracken[7], P.Mendonca, P.Meriguet, P.Micozzi[4], S.F.Mills, P.Millward, S.L.Milora[24], A.Moissonnier, P.L.Mondino, D.Moreau[17], P.Morgan, H.Morsi[14], G.Murphy, M.F.Nave, M.Newman, L.Nickesson, P.Nielsen, P.Noll, W.Obert, D.O'Brien, J.O'Rourke, M.G.Pacco-Düchs, M.Pain, S.Papastergiou, D.Pasini[20], M.Paume[27], N.Peacock[7], D.Pearson[13], F.Pegoraro, M.Pick, S.Pitcher[7], J.Plancoulaine, J-P.Poffé, F.Porcelli, R.Prentice, T.Raimondi, J.Ramette[17], J.M.Rax[27], C.Raymond, P-H.Rebut, J.Removille, F.Rimini, D.Robinson[7], A.Rolfe, R.T.Ross, L.Rossi, G.Rupprecht[14], R.Rushton, P.Rutter, H.C.Sack, G.Sadler, N.Salmon[13], H.Salzmann[14], A.Santagiustina, D.Schissel[25], P.H.Schild, M.Schmid, G.Schmidt[6], R.L.Shaw, A.Sibley, R.Simonini, J.Sips[16], P.Smeulders, J.Snipes, S.Sommers, L.Sonnerup, K.Sonnenberg, M.Stamp, P.Stangeby[19], D.Start, C.A.Steed, D.Stork, P.E.Stott, T.E.Stringer, D.Stubberfield, T.Sugie[18], D.Summers, H.Summers[20], J.Taboda-Duarte[22], J.Tagle[30], H.Tamnen, A.Tanga, A.Taroni, C.Tebaldi[23], A.Tesini, P.R.Thomas, E.Thompson, K.Thomsen[11], P.Trevalion, M.Tschudin, B.Tubbing, K.Uchino[29], E.Usselmann, H.van der Beken, M.von Hellermann, T.Wade, C.Walker, B.A.Wallander, M.Walravens, K.Walter, D.Ward, M.L.Watkins, J.Wesson, D.H.Wheeler, J.Wilks, U.Willen[12], D.Wilson, T.Winkel, C.Woodward, M.Wykes, I.D.Young, L.Zannelli, M.Zarnstorff[6], D.Zasche[14], J.W.Zwart.

PERMANENT ADDRESS

1. UKAEA, Harwell, Oxon. UK.
2. EUR-EB Association, LPP-ERM/KMS, B-1040 Brussels, Belgium.
3. Institute National des Récherches Scientifique, Quebec, Canada.
4. ENEA-CENTRO Di Frascati, I-00044 Frascati, Roma, Italy.
5. Chalmers University of Technology, Göteborg, Sweden.
6. Princeton Plasma Physics Laboratory, New Jersey, USA.
7. UKAEA Culham Laboratory, Abingdon, Oxon. UK.
8. Plasma Physics Laboratory, Space Research Institute, Sao José dos Campos, Brazil.
9. Institute of Mathematics, University of Oxford, UK.
10. CRPP/EPFL, 21 Avenue des Bains, CH-1007 Lausanne, Switzerland.
11. Risø National Laboratory, DK-4000 Roskilde, Denmark.
12. Swedish Energy Research Commission, S-10072 Stockholm, Sweden.
13. Imperial College of Science and Technology, University of London, UK.
14. Max Planck Institut für Plasmaphysik, D-8046 Garching bei München, FRG.
15. Institute for Plasma Research, Gandhinagar Bhat Gujat, India.
16. FOM Instituut voor Plasmafysica, 3430 Be Nieuwegein, The Netherlands.
17. Commissiariat à L'Energie Atomique, F-92260 Fontenay-aux-Roses, France.
18. JAERI, Tokai Research Establishment, Tokai-Mura, Naka-Gun, Japan.
19. Institute for Aerospace Studies, University of Toronto, Downsview, Ontario, Canada.
20. University of Strathclyde, Glasgow, G4 ONG, U.K.
21. Nuclear Engineering Laboratory, Lapeenranta University, Finland.
22. JNICT, Lisboa, Portugal.
23. Department of Mathematics, Univeristy of Bologna, Italy.
24. Oak Ridge National Laboratory, Oak Ridge, Tenn., USA.
25. G.A. Technologies, San Diego, California, USA.
26. Institute for Nuclear Studies, Swierk, Poland.
27. Commissiariat à l'Energie Atomique, Cadarache, France.
28. School of Physical Sciences, Flinders University of South Australia, South Australia SO42.
29. Kyushi University, Kasagu Fukuoka, Japan.
30. Centro de Investigaciones Energeticas Medioambientales y Techalogicas, Spain.
31. University of Maryland, College Park, Maryland, USA.
32. University of Essex, Colchester, UK.
33. Akademie de Wissenschaften, Berlin, DDR.

CR 88.49.1A